THE GEOLOGICAL SOCIETY OF AMERICA®

Three-dimensional strain accumulation and partitioning in an arcuate orogenic wedge: An example from the Himalaya

Suoya Fan†, and Michael A. Murphy
Department of Earth and Atmospheric Sciences, University of Houston, Houston, Texas 77204, USA

ABSTRACT

In this study, we use published geologic maps and cross-sections to construct a three-dimensional geologic model of major shear zones that make up the Himalayan orogenic wedge. The model incorporates microseismicity, megathrust coupling, and various derivatives of the topography to address several questions regarding observed crustal strain patterns and how they are expressed in the landscape. These questions include: (1) How does vertical thickening vary along strike of the orogen? (2) What is the role of oblique convergence in contributing to along-strike thickness variations and the style of deformation? (3) How do variations in the coupling along the megathrust affect the overlying structural style? (4) Do lateral ramps exist along the megathrust? (5) What structural styles underlie and are possibly responsible for the generation of high-elevation, low-relief landscapes? Our model shows that the orogenic core of the western and central Himalaya displays significant along-strike variation in its thickness, from ~25–26 km in the western Himalaya to ~34–42 km in the central Himalaya. The thickness of the orogenic core changes abruptly across the western bounding shear zone of the Gurla Mandhata metamorphic core complex, demonstrating a change in the style of strain there. Pressure-temperature-time results indicate that the thickness of the orogenic core at 37 Ma is 17 km. Assuming this is constant along strike from 81°E to 85°E indicates that, the western and central Nepal Himalaya have been thickened by 0.5 and 1–1.5 times, respectively. West of Gurla Mandhata the orogenic core is significantly thinner and underlies a large 11,000 km² Neogene basin (Zhada). A broad, thick orogenic core associated with thrust duplexing is collocated with an 8500 km² high-elevation, low-relief surface in the Mugu-Dolpa region of west Nepal. We propose that these results can be explained by oblique convergence along a megathrust with an along-strike and down-dip heterogeneous coupling pattern influenced by frontal and oblique ramps along the megathrust.

INTRODUCTION

Studies on the growth of orogenic wedges usually focus on processes normal to the strike of the orogen by assuming plane strain deformation. This assumption is only valid when an orogen is cylindrical and strikes normal to the convergence direction, which is rare or nonexistent in nature. Large orogens extend thousands of kilometers usually change strike and vary in structural style along strike (e.g., Yin, 2006). Thus, studies on three-dimensional (3-D) strain accumulation and partitioning in these orogenic processes are necessary to better understand the effects of oblique convergence and along-strike heterogeneity.

The Himalayan orogenic wedge is arcuate in map view (Bendick and Bilham, 2001). This implies that no sectors of the arc have the same angle of obliquity along its strike (Styron et al., 2011) (Fig. 1), and therefore predicts non-plane-strain conditions along sectors of the orogen that are oblique to the relative plate convergence direction, such as Kumaun and western Nepal Himalaya (McCaffrey, 1992; Platt, 1993).

Early efforts to characterize shear zones comprising the Himalayan orogenic wedge, resulted in establishing the geometry of now regionally recognized first-order features such as the Main Central Thrust (MCT) and South Tibet Detachment System (STD) (e.g., Arita, 1983; Burg et al., 1984; Brunel, 1986; Pêcher, 1989; Schelling and Arita, 1991; Burchfiel et al., 1992; Hodges et al., 1992; Coleman, 1996; Edwards et al., 1996; Carosi et al., 1998). These shear zones can be mapped across the Himalayan wedge for most of its length for >1500 km based on similar juxtaposition of rock sequences and metamorphic grade (e.g., Heim and Gansser, 1939; Gansser, 1964; Le Fort, 1975; Burg and Chen, 1984; Pêcher, 1989). This suggests along-strike continuity in the structural architecture, tectonostratigraphy, and possible evolution. However, several studies have since observed and better understand that significant differences exist (e.g., Paudel and Arita, 2002; Thiede et al., 2006; Yin, 2006; Murphy, 2007; Hintersberger et al., 2010; Webb et al., 2011; Carosi et al., 2013). In the western and central Himalaya, geologic features indicative of different along-strike structural styles and histories comprise thrust duplexes, gneiss domes, and intermontane basins. Two such structures are the Leo Pargil and Gurla Mandhata gneiss domes or metamorphic core complexes in the Kumaun and western Nepal Himalaya, respectively (Fig. 1). Both exhume mid-crustal rock sequences that were located near the Main Himalayan thrust (MHT) prior to their exhumation, thus indicating they are deeply rooted in the wedge. Their development is interpreted to be driven mostly by orogen-parallel stretching (Murphy et al., 2002, 2009; Thiede et al., 2006; Langille et al., 2010b), rather than orogen-normal shear and shortening attributed to the development of the MCT and STD (Srivastava and Mitra, 1994; Webb et al., 2007; Murphy et al., 2009). The Neogene Zhada basin lies between Leo Pargil and Gurla Mandhata and formed on top of their extended hanging walls, thus demonstrating vertical thinning in this region of the orogenic wedge (Murphy et al., 2009; Saylor et al., 2010). Cross-sections across this region illustrate the significant variation in the thickness of the orogenic metamorphic core along the strike (Murphy, 2007; Webb et al., 2011) (Fig. 1). Although the Gurla Mandhata metamorphic core complex (MCC) is mantled by an extensional shear zone, cross-sections across it indicate significant crustal thickening beneath it (Murphy, 2007). Its position in the wedge and geometry suggests that it correlates to the North Himalayan antiform, a series of domes of high-grade metamorphic crystalline rocks that are distributed discontinuously in the hinterland of the northern Himalaya, in southern Tibet. However, these domes do not exhibit

Suoya Fan http://orcid.org/0000-0002-9074-2264
†sfan2@uh.edu.

GSA Bulletin; https://doi.org/10.1130/B35528.1; 6 figures; Data Repository item 2020194.

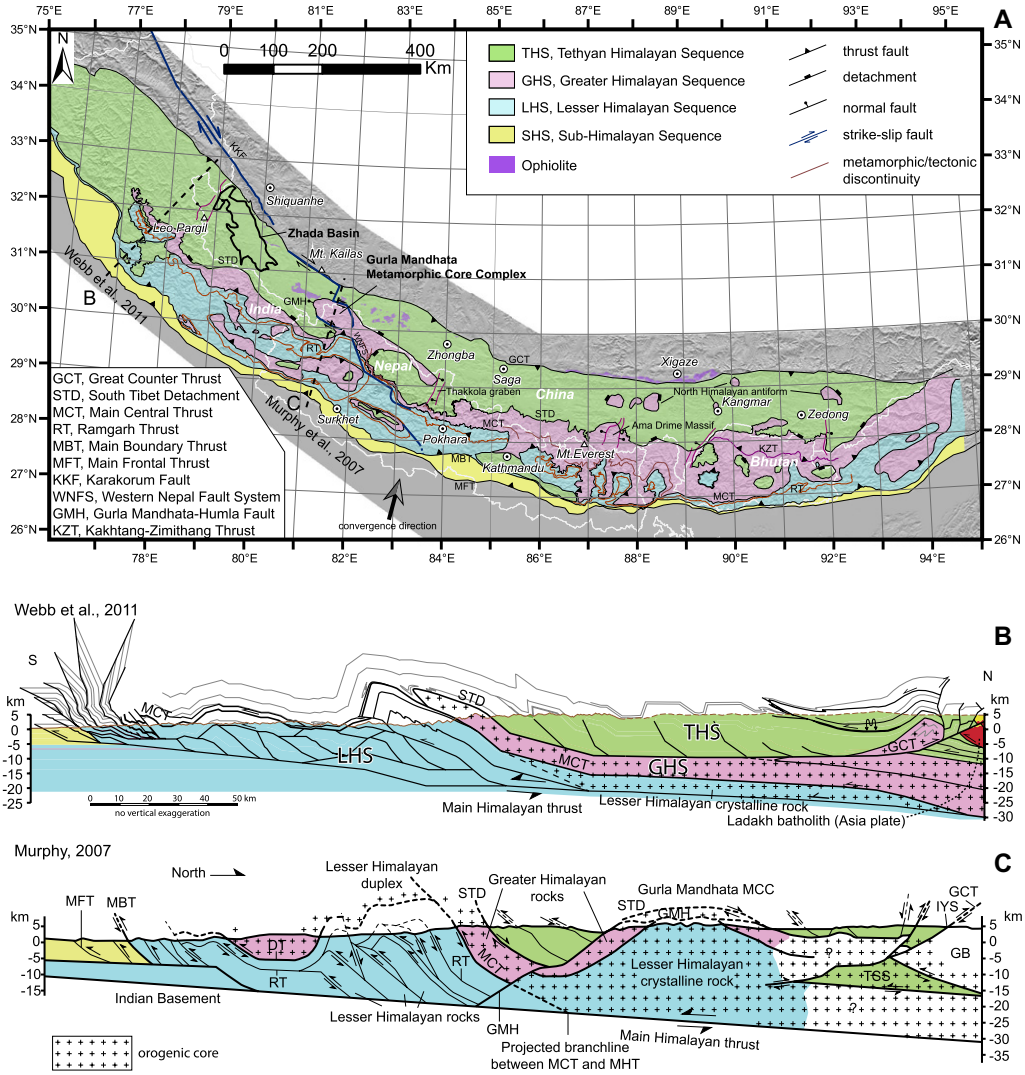

Figure 1. (A) Geologic map of the Himalaya, (B) and (C) are two cross-sections across the western Himalaya (B—Webb et al., 2011; C—Murphy, 2007). The high-grade metamorphosed orogenic core includes the GHS and LHS crystalline rock. Note the difference in the thickness of the orogenic core toward the rear of the orogenic wedge between the two cross-sections.

shear zones that facilitate orogen-parallel shear (e.g., Lee et al., 2000, 2004; Wang et al., 2018; Jessup et al., 2019). These along-strike differences in structure suggest that the Kumaun and Nepal Himalaya is an ideal place to study the 3-D strain accumulation and partitioning in an orogenic system.

To better understand the crustal strain patterns in the Kumaun and western Nepal Himalaya described above and their relationship to that of the central Nepal Himalaya and southern Tibet, we constructed a 3-D geologic model from 76°E to 86°E of three main shear zones bounding the high-grade metamorphic rocks in the Himalaya, the STD on the top, the Main Himalayan Thrust (MHT), and MCT (projected to branch to the MHT) at the bottom (Fig. 1). We use this model to investigate strain accumulation within the orogen. These high-grade metamorphic rocks are usually mapped as the Greater Himalayan sequence (GHS), however, isotopic studies in the Gurla Mandhata MCC in the North Himalaya antiform and the MCT thrust sheet in Bhutan Himalaya indicate material accretion of the Lesser Himalayan sequence (LHS) (Murphy, 2007; Hopkinson et al., 2019). Different from the low-grade metamorphosed LHS mapped to the south of the MCT, these LHS crystalline rock are interpreted to be accreted from the bottom of the wedge in the hinterland and are also experienced high-grade metamorphic conditions. We use the thickness of these high-grade metamorphic rocks as an indicator of accumulated strain in the mid-lower crustal wedge and do not focus on the protolith of the material; therefore, we refer to these high-grade metamorphic rocks, including the high-grade LHS crystalline rock in the hinterland and the GHS, as the "orogenic core" in this paper to avoid confusion (Fig. 1). Moreover, because active brittle fault systems approximately collocate with the shear zones described above at many places, we take this opportunity to address along-strike variations in seismicity patterns, historical earthquake rupture areas, and landscape. This is carried out by integrating our model with independent data sets, including; derivatives of the topography (slope of mean elevation, normalized river steepness, topographic relief), megathrust coupling, seismicity, and thermochronology.

GEOLOGIC BACKGROUND

The base of the Himalayan orogenic wedge is defined by the MHT. The exposed orogenic crystalline core of the Himalaya is bounded by the STD at the top and the MCT at the base (Fig. 1). Although its upper contact is gradational in places, it is generally composed of middle amphibolite facies (kyanite zone) to lower granulite facies meta-sedimentary and meta-igneous rocks with some Oligo–Miocene leucogranites (e.g., Vannay and Hodges, 1996; Searle and Godin, 2003; Martin et al., 2010; Kohn, 2014; Iaccarino et al., 2017). The GHS has long been considered to be a coherent tectonic unit

(see reviews in Yin, 2006). However, in recent studies, several structural and metamorphic "discontinuities" (shear zones) (Montomoli et al., 2013) within the GHS have been reported and interpreted to develop in an in-sequence pattern prior to the initiation of the MCT (see reviews in Larson et al., 2015; Montomoli et al., 2015; Carosi et al., 2018), starting from ca. 41–30 Ma (Carosi et al., 2016). The Tethyan Himalaya sequence (THS) structurally above it is a deformed package of unmetamorphosed to low-grade metasedimentary rocks that experienced maximum green schist to locally amphibolite facies metamorphism (Gaetani and Garzanti, 1991; Burchfiel et al., 1992; Liu and Einsele, 1994; Myrow et al., 2009; Dunkl et al., 2011). Thickening of these rocks after initial collision between India and Asia is shown to be coeval with, and interpreted to drive the first stage of the metamorphism in the Eocene, "Eohimalayan metamorphism," prior to the initiation of the MCT and STD (e.g., Hodges and Silverberg, 1988; Inger and Harris, 1992; Carosi et al., 2015). This metamorphism generated a weakened mid-lower crust. The MCT initiated after that during the late Oligocene–early Miocene (ca. 23–20 Ma) (Kohn et al., 2005; Yin, 2006; Cottle et al., 2015a). The STD is usually interpreted to be coeval with the MCT and ceased moving at ca. 19–16 Ma in Dolpo region, central-western Nepal (Searle and Godin, 2003; Godin et al., 2006; Cottle et al., 2015b), though geochronologic study on a granite in western Nepal suggests the STD ceased moving at 23–25 Ma (Carosi et al., 2013). However, portions of the MCT have been interpreted to have been reactivated in the late Miocene (e.g., Catlos et al., 2001; Braden et al., 2018; Montemagni et al., 2019). Endmember tectonic models accounting for this coeval movement include channel flow (e.g., Beaumont et al., 2001), tectonic wedging (e.g., Yin, 2006; Webb et al., 2011), and wedge extrusion/critical taper (e.g., Burchfiel et al., 1992). Toward the end of the timespan that the STD-MCT system was active (ca. 19–13 Ma), a series of mid-crustal culminations called the North Himalayan antiform developed in the central Himalayan hinterland and southern Tibet exposing the high-grade orogenic core as a series of domes (Fig. 1) (e.g., Lee et al., 2000; Lee and Whitehouse, 2007; Godin et al., 2006; Larson et al., 2010). Structurally below the GHS and MCT is the LHS, bounded by the Main Boundary Thrust (MBT) at the base. It consists of lower-greenschist- to lower-amphibolite-facies clastic metasedimentary rocks. Throughout Nepal and Himachal Himalaya in northwest India, it is structurally involved in a duplex system with a roof thrust identified as the Ramgarh thrust (RT) and Munsiari thrust, respectively (e.g., Srivastava and Mitra, 1994; DeCelles et al., 2001; Pearson and DeCelles, 2005; Robinson et al., 2006; Webb, 2013). Growth of the duplex led to the folding of the MCT structurally above. Erosion of this folded thrust sheet created GHS/THS klippen exposed near the Himalayan thrust front (Fig. 1) (e.g., DeCelles et al., 2001; Pearson and DeCelles, 2005). Duplexing and initiation of the MBT are bracketed to have occurred after displacement on the MCT and estimated to have been active in the late Miocene to Pliocene (DeCelles et al., 1998; Robinson and McQuarrie, 2012). To the south of the MBT, the sub-Himalayan sequence is deformed by the active MFT, which separates these rocks from the Quaternary to modern sediments to the south (Lavé and Avouac, 2000).

The orogenic wedge is also characterized by several fault systems that trend oblique or at a high angle to the strike of the orogen. In the study area these structures include the Leo Pargil MCC and Gurla Mandhata MCC located in the Kumaun Himalaya in India and far-western Nepal, respectively (Murphy and Copeland, 2005; Thiede et al., 2006). In central Nepal, the Thakkhola graben cuts the STD, MCT, and extends into the LHS (Fig. 1). To the east of the study area, the Ama Drime massif is mantled by an extensional shear zone that accommodates orogen parallel extension and exhumes rocks beneath the MCT demonstrating that the shear zone extends deep into the orogenic wedge (Jessup et al., 2008). All these extensional structures initiated around the middle-late Miocene and accommodate orogen-parallel movement (Coleman and Hodges, 1995; Zhang et al., 2000; Murphy et al., 2002; Garzione et al., 2003; Murphy and Copeland, 2005; Thiede et al., 2006; Hintersberger et al., 2010; Langille et al., 2014; McCallister et al., 2014). It is noteworthy that the Zhada basin developed between the two MCCs in the Kumaun Himalaya and temporally overlaps with them in the late Miocene (Wang et al., 2008; Murphy et al., 2009; Saylor et al., 2010). The Karakoram fault is a regionally extensive right-slip fault system at the rear side of the orogenic wedge. It initiated at 25–15 Ma near the Bangong-Nujiang suture zone (Phillips et al., 2004; Valli et al., 2007; Leech, 2008) and propagated southward to the South Kailas area cutting the ca. 13 Ma Great Counter thrust (GCT) (Yin et al., 1999; Murphy et al., 2000; Valli et al., 2007) and accommodates trans-tensional strain in the Ayi Shan area of Tibet at ca. 10.17 Ma (Zhang et al., 2011). The western Nepal fault system (WNFS) is an active strike-slip fault system that obliquely cuts across the orogen and is interpreted to operate as the eastern boundary of a westward translating continental forearc sliver (Murphy et al., 2014; Silver et al., 2015). It is interpreted to connect to the Karakoram fault via the Gurla Mandhata-Humla fault system (GMH), thus forming a regional scale right step-over that accommodates orogen-parallel extension (Murphy et al., 2002; Murphy and Copeland, 2005).

3-D MODEL CONSTRUCTION

Data Sources

To construct the 3-D geologic model, we use published maps, and cross-sections that span the Himalaya from 76°E to 86°E. Where gaps in the spacing between cross-sections were large (>150 km), new cross-sections were constructed. In addition, along-strike cross-sections were constructed to connect adjacent profile interpretations. The locations and references of the published and newly constructed cross-sections are shown in Appendix 1 (Fig. DR1[1]). The MHT is constrained by the seismic profile published by Caldwell et al. (2013) in the Kumaun Himalaya and by the 3-D model published by (Hubbard et al., 2016) for the Nepal region. To convert the map view structures to a 3-D database, we projected the map-view structures onto a Shuttle Radar Topography Mission digital elevation model (DEM).

Method

The 3-D modeling work was carried out using two software programs: ArcGIS and Midland Valley MOVE. ArcGIS was utilized to build a geodatabase consisting of published maps. This allowed us to compile multiple maps in a common projection system and digitize shapefiles for the STD and MCT. They were exported to MOVE and merged with published cross-sections to create a 3-D database. We also digitized the STD and MCT surfaces from cross-sections in MOVE. For the MHT, we reinterpreted the cross-section published in Caldwell et al. (2013) (Fig. DR2 in Appendix 1; see footnote 1) and made it extend along strike of the orogen to the west of Nepal and adopted the 3-D MHT model published in Hubbard et al. (2016) for the Nepal area. All map-view digitized features were projected to the DEM. The lengths of and the space between the cross-sections vary due to the different sizes of the study areas. To better constrain the modeling in the less studied areas, we extended most of the cross-sections to make them straddle the Himalaya thrust wedge and a

[1]GSA Data Repository item 2020194, Appendixes 1–4 (data sources, 3D models, summarized P-T-t data, and supplementary maps), is available at http://www.geosociety.org/datarepository/2020 or by request to editing@geosociety.org.

few new cross-sections were constructed based on the maps and cross-sections in the adjacent areas. When inferring the eroded parts in cross-sections, we tied the structures to the traces from the maps and projected the structures into the air following the geometry based on the structures (e.g., dip of the detachment, fabrics) below it. Finally, we used the kriging algorithm in MOVE to model the MCT and STD surfaces by making the surfaces pass through all the points of corresponding data from both the map view and cross-sections.

RESULTS

Figure 2 shows color-coded elevation maps of the modeled STD, MCT, and MHT (see Fig. DR3 in Appendix 2 for the 3-D view model, see footnote 1). The 3-D view of the geometry of the orogenic core, i.e., the space bounded by the STD from the top, the MCT and MHT from the bottom at the frontal part and hinterland part, respectively, is shown in Appendix 2 (Fig. DR3). The STD model exhibits significant structural relief, as much as ~34 km. The lowest area is in the western Himalaya between the Leo Pargil dome and the Gurla Mandhata MCC, where the Zhada basin is located. The highest part is to the south of the Gurla Mandhata MCC, which is caused by the duplexing in the LHS structurally below the GHS.

To investigate the strain accumulated in the orogenic core, we calculated its thickness by using the modeled elevation data of the STD, MCT, and MHT (Fig. 2D). The thickness of the core is the elevation difference between the STD and MCT for the frontal part and the difference between the STD and MHT for the hinterland part. The thickness map shows significant along-strike variation in thickness in the hinterland, increasing from ~25–26 km in the western Himalaya to ~34–42 km in the central Himalaya. The along-strike abrupt change is at the GMH, which accommodated orogen-parallel extension and is where the strike of the orogen changes from NWW to NW. The thinnest part in the hinterland is under the Zhada basin, which is interpreted to be a pull-apart or supradetachment basin caused by orogen-parallel extension and tectonic damming (Murphy et al., 2009; Saylor et al., 2010).

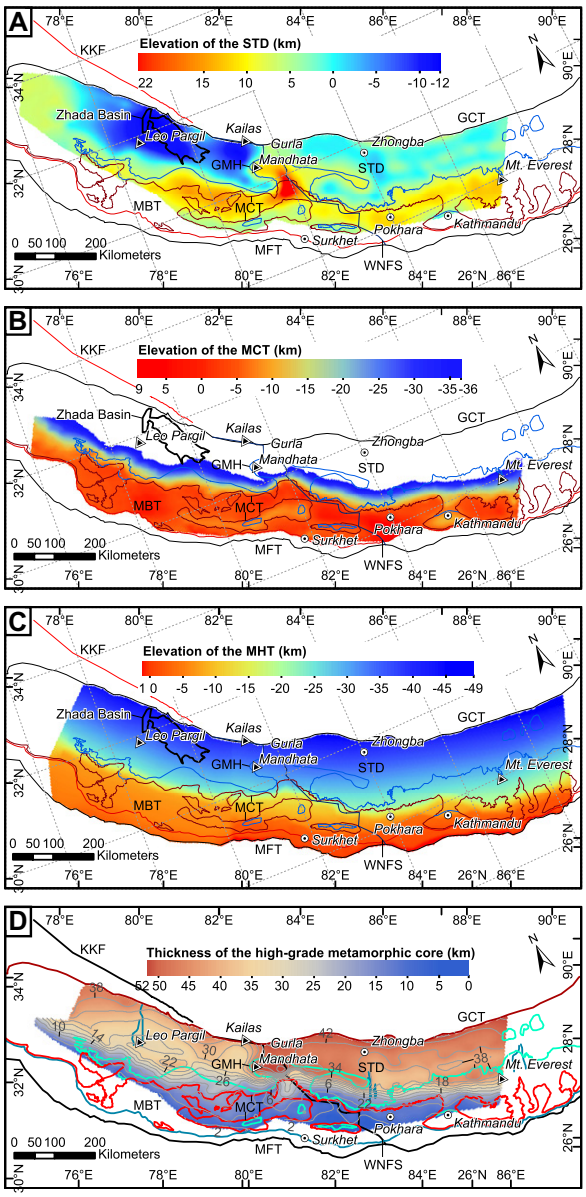

Figure 2. (A, B, and C) are color-coded elevation maps of the modeled 3-D surfaces of the South Tibet Detachment System (STD), Main Central Thrust (MCT), and Main Himalayan Thrust (MHT), respectively. (D) is a color-coded thickness map of the high-grade orogenic core of the western and central Himalaya. The gray lines labeled with numbers are thickness contours (in kilometer). Also shown are surface traces of major shear zones. See abbreviations in Figure 1A.

DISCUSSION

Along-Strike Strain Variation

In this section, we evaluate the thickness variations of the orogenic core portrayed in our geologic model. We assume that the modeled (present-day) thickness is an indicator of how much strain has accumulated in the mid-lower crust during Himalayan orogenesis. The greatest challenge in estimating strain based on the current thickness of the orogenic core is establishing its thickness at a particular time. The thickness of the orogenic core in the past is poorly understood due to the overprinting of younger deformation and an incomplete record of shortening and timing estimates of shear zones within it. Nevertheless, we attempt to estimate along-strike strain variations, by using the "Eohimalayan metamorphism" stage as the initial state. We chose this event because it occurred prior to movement on the major structures recognized that involve the orogenic core and thus the core might have had much less along-strike variation in thickness than today. We outline the basis for this assumption.

Although there are few published shortening estimates, the THS is estimated to have undergone between 30% and 70% horizontal shortening (Ratschbacher et al., 1994; Vannay and Steck, 1995; Godin et al., 1999; Murphy and Yin, 2003). These estimates do not include shortening due to Miocene slip along the GCT that locally defines the surface trace of the India-Asia suture zone (Yin et al., 1994; Quidelleur et al., 1997). Cenozoic shortening of the THS is interpreted to be widespread, based on the correlation of structural styles and regionally recognized structures, such as the Kangmar-Gyirong-Lhunze fault (Aikman et al., 2008). Disregarding Miocene shortening along the suture, the timing of crustal shortening is bracketed to have occurred during the Eocene (Ratschbacher et al., 1994; Wiesmayr and Grasemann, 2002; Ding et al.,

2005; Aikman et al., 2008). The high-grade metamorphosed orogenic core is interpreted to have been metamorphosed during this period of crustal thickening (Vannay and Hodges, 1996). This metamorphic event predates movement along the STD, MCT, and the younger thrusts to the south and structurally beneath them and is referred as "Eohimalayan metamorphism" to distinguish it from "Neohimalayan metamorphism" later. Therefore, neither significant strain nor along-strike variation in the thickness of orogenic core is likely to have been caused by structures below the THS during Eohimalayan metamorphism.

The minimum possible depth of the MHT during Eohimalayan metamorphism could be understood by the peak metamorphic conditions of the exposed rocks. In the Kali Gandaki area, the estimated peak metamorphic conditions are 610 °C and 940 MPa (>35 km). Hornblende $^{40}Ar/^{39}Ar$ dating on the same sample yields an age of 37.2 ± 2.8 Ma and is interpreted as the age of amphibolite facies metamorphism during the Eohimalayan stage (Vannay and Hodges, 1996). This is in agreement with a study on nanogranites in garnet suggesting partial melting of the GHS, required in the formation of a weak lower crust, initiated at ca. 41–36 Ma (Carosi et al., 2015). Studies on Eohimalayan metamorphism in other areas, except for the orogenic syntaxis, report similar results (Table DR1 in Appendix 3, see footnote 1): most of the estimated peak pressure is as high as 1 Gpa (~37 km) and metamorphic ages are generally late Eocene (Hodges et al., 1996; Coleman and Hodges, 1998; Catlos et al., 2001, 2002; Yakymchuk and Godin, 2012; Carosi et al., 2016). A couple of studies in central and eastern Nepal reported peak P as high as 1.1 Gpa (Catlos et al., 2002; Iaccarino et al., 2015), but it is unclear if this variation in peak metamorphic condition is caused by a variation in the MHT depth or by a lack of information on rocks from deeper depth in other areas. Assuming the rock density is 2.7 kg/m^3, the former possibility could account for variation in the thickness of the core as much as ~3.7 km, less than ~30% of the present variation in thickness of the hinterland core. The latter possibility can only bring in the uncertainty in the total strain estimation but cannot affect the estimation of the amount of thickening. Therefore, the difference of the peak P data cannot alone account for the general trend observed. Collectively, pressure, temperature, and timing estimates indicate that the minimum depth of the MHT at ca. 37 Ma was ~37 km (peak metamorphic pressure ≥1 Gpa).

The initial depth of the upper bounding detachment of the core, STD, could be estimated based on the metamorphic conditions and deformation temperatures of the rocks close to it. The reported minimum peak metamorphic temperature of the rocks at the base of the detachment and directly below the STD reaches 600–650 °C (e.g., Hodges et al., 1992; Pognante and Benna, 1993; Searle, 1999; Searle et al., 2003; Kellett et al., 2010; Cottle et al., 2011). Since the orogenic core experienced extensional non-coaxial flow strain characterized by a higher simple shear component close to the STD (Law et al., 2004, 2013; Carosi et al., 2006, 2007; Jessup et al., 2006; Larson and Godin, 2009; Langille et al., 2010a; Parsons et al., 2016), these peak temperatures should be higher than the temperature of the rocks within the STD at its initiation, i.e., the STD initiated at a temperature lower than ~600 °C. This is also implied by an abrupt increase of the temperature determined by Raman spectroscopy of carbonaceous rocks, from 421 to 450 °C to higher than 600 °C downsection within several hundred meters in the STD shear zone (Cooper et al., 2013; Kellett and Grujic, 2012; Long et al., 2019). Deformation temperatures along three transects determined by quartz c-axis fabrics measured on dynamically recrystallized quartz also show a gradual increase from ~490–540 °C within 10–20 m below the STD to 625–680 °C at 420–560 m beneath the STD (Law et al., 2011). Collectively, the STD might have initiated and continuously been active approximately at the depth of the 500 °C isotherm. The thermal structure in the past is not well-known, because it is sensitive to the contemporary megathrust kinematics as suggested by thermo-kinematic modeling (Whipp and Ehlers, 2007; Célérier et al., 2009; Herman et al., 2010; Coutand et al., 2014; Landry et al., 2016). However, these modeling studies report a set of models that could predict cooling ages that match well with observed cooling ages from various dating methods. The thermal structures of these models suggest that a geothermal gradient of ~25 °C/km is a reasonable assumption for the upper at least 30 km of the overthrusting plate. Considering that the STD initiated around the ~500 °C isotherm, as discussed earlier, it is estimated that the depth of the STD in the Eocene was ~20 km.

Therefore, the estimated depths of the MHT and STD lead to an assumption that the thickness of the orogenic core was ~17 km at ca. 37 Ma. Using our model results for present-day thickness of ~25–26 km in the western Himalaya to ~34–42 km in the central Himalaya, we estimate the orogenic core between 83°E and 86°E has been thickened by 1–1.5 times. The thickest part, at the Gurla Mandhata MCC, has been thickened by ~2 times. To the west of the Gurla Mandhata MCC, the orogenic core has only been thickened by ~0.5 times. This region corresponds to the Zhada basin.

Oblique Convergence

Any model describing deformation of the orogenic wedge should account for the significant thickness variation described above and shown in Figure 2D.

Here we attempt to reconcile the thickness variation with a model describing oblique convergence (Fig. 3) (e.g., McCaffrey and Nabelek, 1998; Murphy and Copeland, 2005; Styron et al., 2011). The Himalayan orogen is arcuate in map-view. Geodynamic modeling results show that oblique convergence in the arcuate western Himalaya could generate along-strike material transfer and a gradient in the rate (Whipp and Beaumont, 2016). This supports the model setup shown in Figure 3 whereby the orogen between 76°E and 86°E is be divided into two segments of different strain states; an approximately convergence-orthogonal eastern sector striking EW and an arcuate convergence-oblique western sector striking NW-SE (Fig. 3A). In this conceptual model the convergence-orthogonal segment in the central Himalaya is only subject to orogen-normal (ON) convergence (Fig. 3B). Studies in this region report thrust-sense shear zones within the GHS, which have been interpreted to be part of a duplex in the mid-lower crust (see reviews in Larson et al., 2015; Carosi et al., 2018 and references therein). Large duplexes have also been interpreted in deep-seismic reflection profiles along several transects including the Gurla Mandhata area (Gao et al., 2016; Guo et al., 2017; Laskowski et al., 2018). Although the shear zones identified within the GHS on the surface have been interpreted to be older than the MCT (e.g., Carosi et al., 2018), duplexing might have intermittently been accommodating mid-lower crust thickening to the present (will be discussed later). The identified shear zones within the GHS on the surface are representatives of an exhumed older duplex that formed in the mid-lower crust. The oblique convergence in the west is partitioned into orogen-normal (ON) and orogen-parallel (OP) components. The OP component of the dragging force of the MHT on the upper plate causes OP extension that competes with the shortening/thickening effect of the ON component. As the obliquity of the convergence increases to the west along the strike of the orogen, the magnitude of the OP component of the dragging force increases and the magnitude of the ON component decreases (Fig. 3). This along-strike gradient is supported by analysis of global positioning system velocities, which shows a 2-fold increase in the OP velocity between far-western Nepal and the Kumaun Himalaya (Styron et al., 2011). This is viewed as the cause for internal OP stretching of the orogenic wedge in our model. Others

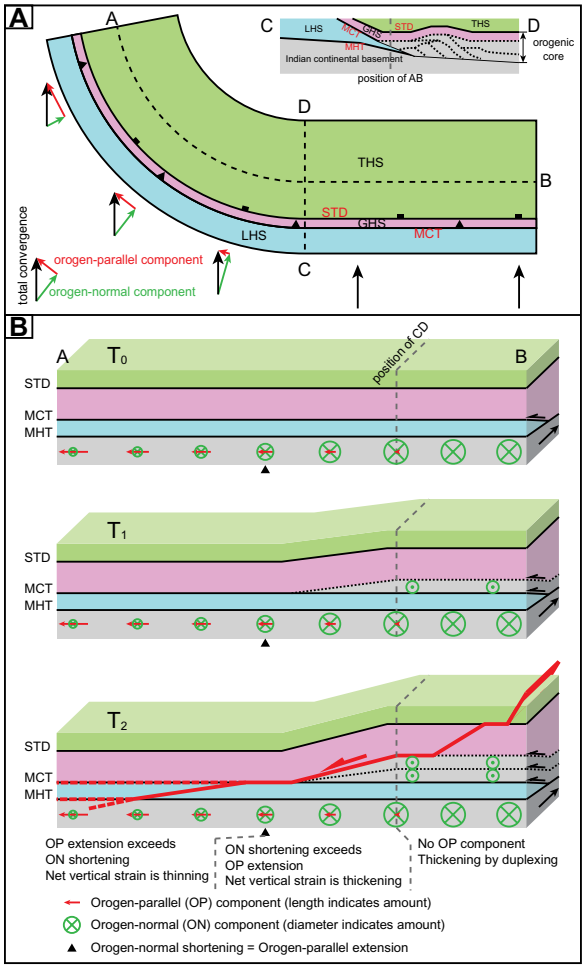

Figure 3. Schematic model of oblique convergence of the western and central Himalaya. (A) shows a schematic map of the convergent setting with western sector oblique and eastern sector orthogonal to the convergence. In the oblique segment, convergence (black arrows) is partitioned into orogen-parallel (OP) component (red arrows) and orogen-normal (ON) component (green arrows). The top-right schematic cross-section shows the general structure of the orogenic wedge. (B) Block diagrams with an orogen-parallel cross-section (AB) in the front showing structural evolution of the orogenic wedge. In the convergence-orthogonal sector, strain has only ON shortening component and is accommodated by duplexing at the brittle-ductile transition zone along the Main Himalayan Thrust (MHT). In the oblique sector, OP extension increases, and ON shortening decrease westward as obliquity increases. Once the extensional component exceeds the thickening component (at black triangle in the figure), the net vertical strain is thinning. Regional OP extensional detachment (e.g., GMH) could develop between the orthogonal and oblique sectors by connecting preexisting structures including the top and edge of the duplex formed in the thickening part, to accommodate the along-strike strain variation. Supra-detachment basin (e.g., Zhada basin) could develop where net vertical strain is thinning. GHS—Greater Himalayan sequence; LHS—Lesser Himalayan sequence; MCT—Main Central Thrust; STD—South Tibet Detachment; THS—Tethyan Himalayan sequence.

have interpreted that this region of the Himalayas behaves as a continental version of a forearc sliver (Murphy et al., 2014). The model presented here implies that this forearc sliver is internally stretched as well as translated to the northwest as suggested by Kundu et al. (2014). According to the model there should be a unique position in the convergence-oblique sector, here referred to as the neutral position, where the amount of thickening caused by the ON shortening equals the amount of thinning caused by the OP stretching, i.e., the vertical net strain is 0 (Fig. 3B). To the east of the neutral position, ON shortening strain exceeds OP stretching strain and the net vertical strain is thickening. This region corresponds to the Gurla Mandhata area, which is characterized by the thickest part of the orogenic core modeled in this study. To the west of the neutral position, OP stretching strain exceeds ON shortening and the net vertical strain is thinning. This region corresponds to the Zhada basin which records a decrease in the mean watershed elevation of 1–1.5 km since then (Murphy et al., 2009; Saylor et al., 2009; Huntington et al., 2015). The subsidence history of the Zhada basin suggests that it is a pull-apart basin type but with a relatively very low-subsidence rate compared with classical pull-apart basins (Saylor et al., 2010). The basin formed during the late Miocene (Wang et al., 2008; Saylor et al., 2010) and lies between the Leo Pargil massif and the Gurla Mandhata MCC. The Leo Pargil massif is bounded by two NE-SW–striking extensional shear zones. The western bounding detachment is the top-to-the-NW Leo Pargil shear zone. West-plunging mineral stretching lineations are well-preserved in the footwall of the Leo Pargil shear zone (Thiede et al., 2006; Hintersberger et al., 2010; Langille et al., 2014). The eastern bounding Qusum detachment is top-to SE and dips moderately to the SE with a mean slip direction of S30E (Murphy et al., 2009). This style of extension (opposing shear zones) suggests NW-SE horizontal coaxial stretching in this region (Fig. 3B). The GMH bounds the Zhada basin along its southeast margin and is interpreted as an extensional step-over connecting the Karakoram fault to the WNFS. It consists of two top-to-west extensional shear zones and locally coincides with the STD. Mineral stretching lineations and shear sense indicators along the detachment and within the mylonitic lower plate of the Gurla Mandhata MCC indicate EW to WNW-ESE–shearing (Murphy et al., 2009; Xu et al., 2013; Nagy et al., 2015). These features indicate that non-coaxial shearing at mid-upper crustal levels accommodated OP extension along the margins of the Zhada basin during its development. This is consistent with the non-coaxial flow strain pattern documented in the high-grade metamorphic core in its front (the MCT thrust sheet): The ductile strain in the high-grade orogenic core is a combination of the pure-shear extension and simple shear. The pure shear component increases toward the interior of the GHS and the simple shear component increase toward the bounding shear zones (Law et al., 2004; Carosi et al., 2006, 2007; Jessup et al., 2006; Larson and Godin, 2009; Langille et al., 2010a; Law et al., 2013; Parsons et al., 2016). But different from the frontal part of the core, where most of these studies were conducted, the net strain in the hinterland is still thickening, because mid-lower crustal material accretion (will be discussed later) has compensated the thinning effect of the non-coaxial flow strain.

In a duplex structure, a local extensional setting could form along the culmination walls or the lateral edges bounding the thickened area (Butler, 1982a, 1982b; Adams et al., 2013). Similarly, the variation of the net vertical strain state between the convergence orthogonal segment and the oblique segment can generate OP extensional shear sense between the two segments in the upper crust (Fig. 3B). This is consistent with the development of the GMH, a large-scale extensional fault system, at the position of the abrupt along-strike change in the thickness of the orogenic core (Fig. 2D). Earth surface studies and seismic reflection profiles in many areas have shown that it is common for shear zones at shallow depth to connect to sub-horizontal detachments at mid-lower crustal depth (e.g., Lemiszki and Brown, 1988; Jones et al., 1992; Hajnal et al., 1996; Jolivet et al., 2001, 2004; Lavier and Manatschal, 2006;

Wang et al., 2011; Clerc et al., 2015). Therefore, the shear within the Gurla Mandhata MCC and the Qusum detachment could be kinematically linked to sub-horizontal shear zones in the lower crust below the Zhada basin, making the geometry and subsidence of the basin more similar to a supra-detachment basin (Friedmann and Burbank, 1995; Saylor et al., 2010) (Fig. 3B). This explains that the greatest crustal thinning and therefore the largest subsidence at the center of the basin and not at the edge surface traces of the basin-bounding faults (Saylor et al., 2010). The depth and low dip of this hypothesized detachment may be a cause for the low subsidence rate of the Zhada basin, though it could also be explained by that the OP extension at the Zhada basin area is partially compensated by the coeval ON shortening (Fig. 3B). The GMH could be connected to sub-horizontal shear zones at depth located along pre-existing and developing weak zones, such as the top and edge of the duplex structures as well as south-directed major thrusts in the orogenic wedge (Fig. 3B). Similarly, the formation of WNFS could also exploit these pre-existing weak zones. This fault-developing mechanism is suggested by the coincidence between the surface traces of the GMH and STD in Gurla Mandhata area, and between the WNFS and MCT or RT (Fig. 1).

Initiation of Strain Partitioning and Mechanisms

What initiated strain partitioning? As described earlier, structures that accommodate strain partitioning in the orogenic wedge did not develop until the middle-late Miocene (e.g., Murphy et al., 2009). These include the GMH, Leo Pargil shear zone, and the Karakoram fault. Prior to this, crustal shortening and thickening dominated deformation at the rear of the wedge. Shortening was accommodated mostly by the GCT (Yin et al., 1999), but may have extended northwards into the Gangdese batholith as recognized by Laskowski et al. (2018) further to the east near Saga County, Tibet (Fig. 1). The region of thickened crust is interpreted to extend southwards from the suture zone to the southern margin of Zhada basin. The transition from no partitioning to partitioning of upper crust convergent thickening to orogen parallel extension is represented by the development of extensional shear zones and strike-slip fault systems that accommodate slip in a direction parallel to the local strike of the orogen. The ductile fabrics record high-temperature ductile OP stretching in the early-middle Miocene, which is well bracketed by monazite U-Pb ages and muscovite $^{40}Ar/^{39}Ar$ ages (Murphy et al., 2002; Thiede et al., 2006; Langille et al., 2012; Xu et al., 2013; McCallister et al., 2014; Nagy et al., 2015). Conceptually, orogen-parallel extension within an active orogenic wedge implies that the orogenic core could still be thickening by continuous accretion of material at the bottom of the wedge in middle and lower crust. The upper crustal extension or OP partition did not initiate until middle-late Miocene in the western Himalaya, recorded by dome exhumation, basin formation, and topographic inversion (e.g., Pêcher et al., 1991; Murphy et al., 2002, 2009; Thiede et al., 2006; Saylor et al., 2010; Xu et al., 2013; McCallister et al., 2014; Nagy et al., 2015; Parsons et al., 2016). Rapid cooling of the Leo Pargil high-grade metamorphic rocks occurred between 12 and 16 Ma (Zhang et al., 2000; Thiede et al., 2006; Hintersberger et al., 2010; Thöni et al., 2012). The initiation of the GMH is 9–15 Ma (Murphy et al., 2002; Murphy and Copeland, 2005; McCallister et al., 2014). The subsidence of the Zhada basin area started at ca. 9.5 Ma (Wang et al., 2008; Saylor et al., 2010). This raises another question, what initiated upper crustal OP extension and strain partitioning in the western Himalaya during the middle-late Miocene.

One possible trigger could be an increase in obliquity of the western Himalayan convergence in middle-late Miocene. Models of oblique convergence suggest that only when the obliquity of convergence increases to a certain value can strain partitioning occur via the formation of a strike-slip fault at the rear of the orogenic wedge to accommodate the OP strain (McCaffrey, 1992; Platt, 1993). When and how the Himalaya orogen obtained the arcuate shape have been discussed in some paleomagnetic studies. These studies have detected rotation between different units or areas suggesting that oroclinal bending or rotational thrusting is an important process in the Miocene (Klootwijk et al., 1985; Schill et al., 2001, 2002, 2004; Crouzet et al., 2003). Although Schill et al. (2001, 2002, 2004) argue specifically that most of the rotational thrusting or oroclinal bending was accommodated by structures to the south of the LHS, which did not initiate until late Miocene to Pliocene (Meigs et al., 1995; DeCelles et al., 1998), their relative rotation data is of high uncertainty (usually >100%). Therefore, it is likely that the increased convergent obliquity in western Himalaya in the Miocene could have triggered upper crustal OP extensional strain partitioning.

The other possible cause is development of a weak backstop to the western margin of the orogenic wedge in the middle-late Miocene. Geodynamic modeling results show that OP material translation is generated in the western Himalaya only when the rear side of the wedge is weak (Whipp et al., 2014). Without a preexisting weak rear, the orogenic wedge only accommodates shortening strain and material does not translate along strike. This is consistent with the geologic observations at the rear of the wedge. Field mapping of the GCT in southwestern Tibet and thermochronology of the Kailas conglomerate in its footwall suggest initiation of the GCT at the rear of the wedge during the early-middle Miocene (18–13 Ma) (Yin et al., 1999; DeCelles et al., 2011; Zhang et al., 2011). The GCT is cut by the Karakoram fault in southwestern Tibet, indicating a transition from thrusting to strike-slip faulting at the rear of the wedge after 18–13 Ma (Murphy et al., 2000). This is consistent with the $^{40}Ar/^{39}Ar$ muscovite age of 10 Ma in Ayi Shan area which is interpreted to result from exhumation of the Ayi Shan by normal dip slip along the Karakoram fault (Zhang et al., 2011). The existence of the geothermal springs along the Karakoram fault and their high $^{3}He/^{4}He$ ratio suggest mantle fluids flow within the Karakoram fault, supporting a weakened rear of the wedge (Klemperer et al., 2013). Following Whipp et al. (2014) we interpret this transition from thrusting to strike-slip faulting to reflect a shift from a strong to weak rear side of the Himalayan wedge and therefore a change to strain partitioning of the western portion of the Himalayan wedge in the late Miocene. Formation of weak rear back and increase in convergent obliquity are not necessarily exclusive with each other in explaining the initiation of OP strain partition. The development of strike-slip faults at the rear side of the orogen could be the result of the increased convergent obliquity (Platt, 1993).

Rheology of the MHT and Wedge Growth

Oblique convergence can explain the first-order observation that the Kumaun Himalaya accumulated less net vertical thickening than the Nepal Himalaya and the formation of orogen-parallel extensional features in the oblique western segment, such as releasing bend basins, extensional shear zones, and MCCs. However, this model predicts that the central part of the orogeny in central Nepal should have accumulated the largest net vertical thickening strain due to zero OP strain partitioning, whereas the thickest part of the orogenic core is in the Gurla Mandhata area. We suggest that this "anomaly" in the thickness could be caused by the along strike variations in the geometry and rheology of the MHT.

The location of the seismogenic zone at subduction zones is thought to be controlled by the rheology of the subduction interface at the brittle-plastic transition zone or downward limit of the strongly coupled area (Hyndman et al., 1997; Oleskevich et al., 1999). On the surface, this position is represented by a slope break in

the wedge topography, such as the coastline, continental shelf, or forearc high (Ruff and Tichelaar, 1996; Fuller et al., 2006; Wang and Hu, 2006; Malatesta et al., 2018). Numerical and geodetically constrained models also suggest a greater uplift rate above the brittle-ductile transition zone due to strain accumulation at this location (e.g., Fuller et al., 2006; Malatesta et al., 2018). The same mechanism of strain accumulation may also be applicable to the Himalayan orogenic wedge as indicated by several studies. Geodetic and seismic data and numerical modeling in the Himalaya show that a zone of interseismic-localized uplift is collocated with intense microseimic activity and the base of the strongly coupled zone along the megathrust, and suggest that creeping shear at the base of the brittle-ductile zone in mid-lower crust works as the strain reservoir in strain accumulation (Pandey et al., 1995; Bilham et al., 1997; Cattin and Avouac, 2000; Stevens and Avouac, 2015; Mencin et al., 2016). Derivatives of the topography including normalized channel steepness (*Ksn*) and the slope of the mean elevation are usually interpreted to be indicators of rock uplift rate or activity of structures over a time scale of 10^4–10^5 years (Kirby and Whipple, 2001; Wobus et al., 2006; Cannon and Murphy, 2014; Harvey et al., 2015; Adams et al., 2016; Whipple et al., 2016; Cannon et al., 2018; Eizenhöfer et al., 2019). The coincidence between the zone of intense microseimic activity and other longer-time-scale features, such as the high topographic front (the front of the high-elevation, low-relief landscape), high slope of mean elevation (slope break), high river *Ksn*, rocks of young low-temperature thermochronologic ages, and the general pattern of the GHS (trace of MCT) (Fig. 4 and Fig. DR4 in Appendix 4, see footnote 1), further suggests that the location of localized strain accumulation or brittle-ductile transition zone along the megathrust has not moved much in the past several millions of years. The stable state could be a consequence of the dynamic balance between concentrated erosion at the front of the localized uplifting zone and strain accumulation at the base of brittle-ductile transition zone along the MHT (Avouac and Burov, 1996; Lavé and Avouac, 2001; Burbank et al., 2003). Similar to the late Miocene LHS duplexing, functioning to thicken the upper crust (e.g., Srivastava and Mitra, 1994; DeCelles et al., 2001; Robinson et al., 2006; McQuarrie et al., 2008; Robinson and Martin, 2014; Mendoza et al., 2019), ductile duplexing along the brittle-ductile transition zone might have been the mechanism of thickening the orogenic core in the mid-lower crust. It is supported by estimated pressure-temperature conditions and kinematics along "discontinuities" within the GHS (see review in Larson

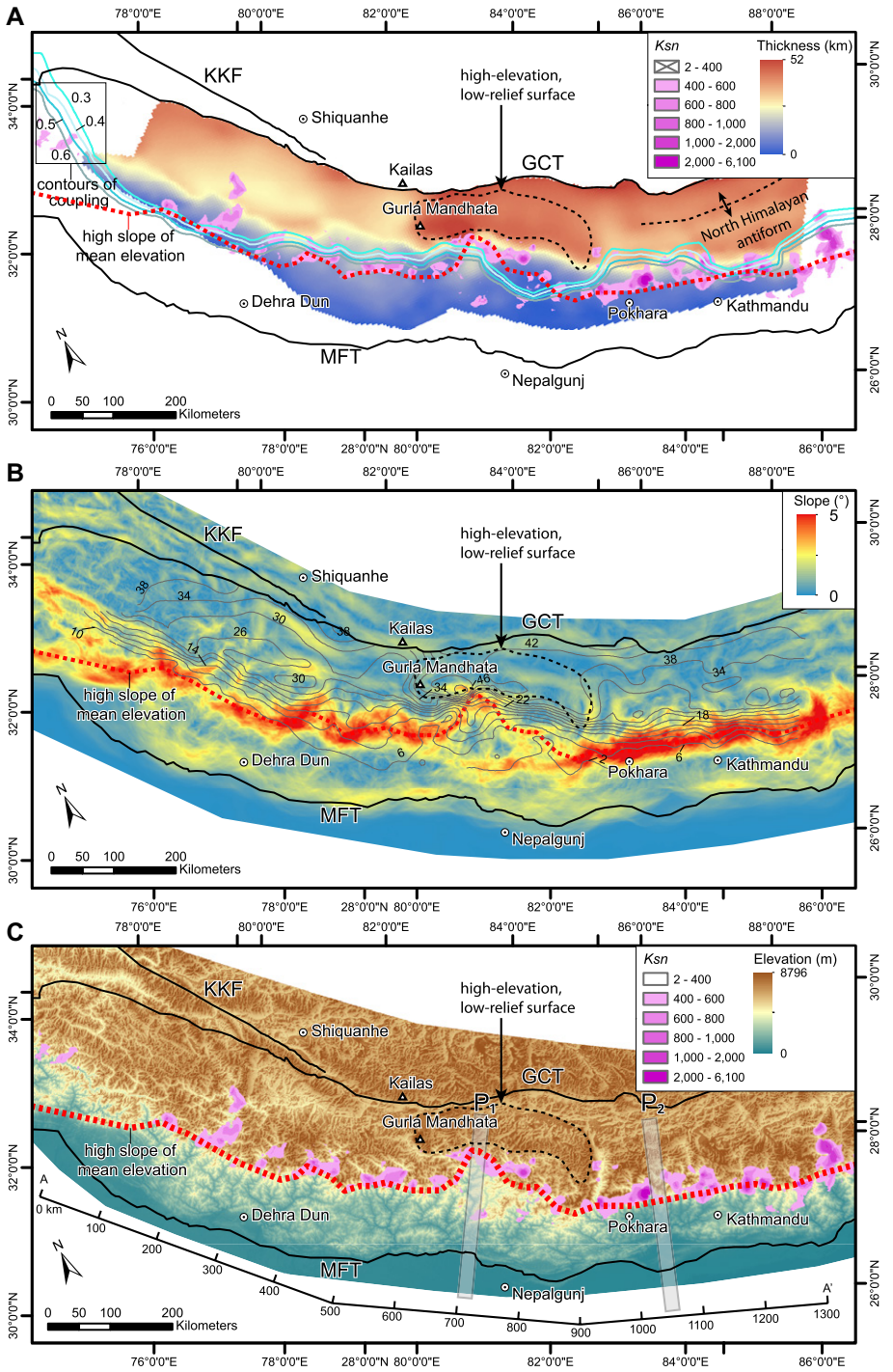

Figure 4. Maps comparing the thickness of the high-grade orogenic core of the western and central Himalaya (color-coded base map in A and gray thickness contours, in km, in B), high slope of mean elevation (color-coded base map in B and red dash lines in A, B, and C), contoured areas of high normalized river channel steepness (K_{sn}) (purple clusters in A and C, from Cannon et al., 2018), modeled coupling of the Main Himalayan Thrust (contours of 0.3–0.6 in A, from Stevens and Avouac, 2015). Slope of mean elevation was calculated by first smoothing the topography by taking the mean within a 25 km moving window and then calculating the slope of the resulting grid. Notice the correspondence between the patterns of these features and their along-strike anomaly between 81°E and 83°E. KKF—Karakorum fault; GCT—Great Counter Thrust; MFT—Main Frontal Thrust. P_1 and P_2 show locations of two topographic swath profiles presented in Figure 5.

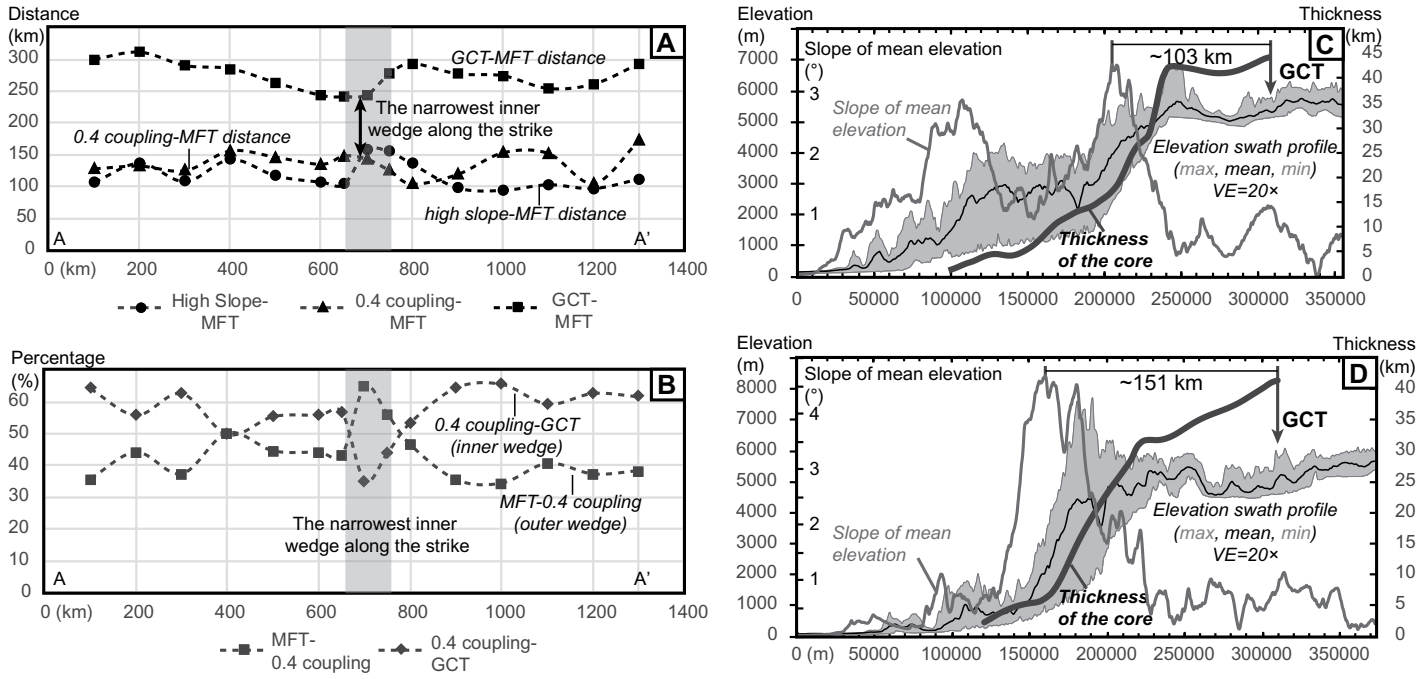

Figure 5. Plots of multiple datasets exhibit along-strike variations in the western and central Himalayan orogenic wedge. (A) Along-strike change in the distances between the Main Frontal Thrust (MFT), 0.4 MHT coupling contour, interpreted high slope zone, and the Great Counter Thrust (GCT), and (B) percentage of the outer wedge (distance between MFT and 0.4 MHT coupling contour) and the inner wedge (distance between 0.4 MHT coupling contour and GCT) in the total width of the orogenic wedge (distance between MFT and GCT). Dots represent measured data. Horizontal axis represents the distance along the strike of the Himalaya (measured along AA' in Fig. 4C). (C) and (D) are two topographic swath profiles (western Dolpo area, P_1 and central Nepal, P_2) plotted with profiles of thickness of the orogenic core and slope of mean elevation. VE—vertical exaggeration.

et al., 2015), underplating processes suggested by isotopic signatures of the crystalline rocks (Murphy, 2007; Hopkinson et al., 2019), seismic reflection profiles (e.g., Gao et al., 2016; Guo et al., 2018; Laskowski et al., 2018), thermokinematic modeling of the Himalaya (e.g., Bollinger et al., 2006; Herman et al., 2010), tilting amount and history of tectonic thrust sheets in the Himalaya (Schill et al., 2004), and geomorphologic modeling of high-elevation, low-relief landscapes (Adams et al., 2016).

As the rheology of the megathrust is a complex function of a variety of parameters such as its geometry, depth, fluids present, thermal structure, and composition, the location of the brittle-ductile transition zone usually varies along strike of the wedge (e.g., Pacheco et al., 1993; Oleskevich et al., 1999; Klotz et al., 2001; Flórez-Rodríguez et al., 2019; Suenaga et al., 2019). Similarly, the anomaly of the thickness of the orogenic core mentioned above can also be explained by the heterogeneity of the megathrust rheology along strike. Along the strike of the Himalaya, the location of the brittle-ductile transition zone along the MHT or the uplifting front is clear except for far-western Nepal. In far-western Nepal, zones of high river *Ksn* and high slope of mean elevation bifurcate into two branches to the southeast of the Gurla Mandhata MCC (Harvey et al., 2015; Cannon et al., 2018) (Fig. 4). The seismicity is less concentrated and forms a wider zone between the two branches (Fig. DR4). We interpret the northern branch as an active oblique thrust ramp because it coincides with the front of high-elevation, low-relief landscape and area of high exhumation rate as suggested by the young thermochronologic ages from a variety of dating methods including zircon and apatite (U-Th)/He, zircon and apatite fission track, and muscovite $^{40}Ar/^{39}Ar$ (Fig. DR4). The active front forms a structural and topographic embayment in far-western Nepal, suggesting that the brittle-ductile transition zone along the MHT is farther north in far-western Nepal compared to the adjacent regions along strike. This is also supported by the northward shift of the strongly coupled part of MHT (Fig. 4) (Ader et al., 2012; Stevens and Avouac, 2015). This embayment-like feature places the active lower-crustal duplexing in far-western Nepal approximately at the southern edge of Gurla Mandhata MCC (North Himalayan antiform), whereas the active uplifting front to the east in the central Himalaya is usually more than 100 km to the south of the North Himalayan antiform (Fig. 4). Along strike of the Himalaya, the Gurla Mandhata MCC sector (~600–700 m along AA' in Fig. 4C) also has the narrowest orogenic wedge (distance between the MFT and GCT) and the smallest proportion of the inner wedge (represented by the 0.4 MHT coupling contour line and the GCT) (Figs. 5A and 5B). The present active uplifting front represents the southernmost limit of the mid-lower crustal duplexing in the orogenic core thickening process. Therefore, the shortening strain caused by lower-crustal duplexing in the Gurla Mandhata area accumulated within a relatively narrower zone than in the central Nepal Himalaya, where the thickening of the orogenic core is less concentrated (Fig. 5). The focused thickening through time in far-western Nepal provides an explanation for why the Gurla Mandhata area and not the central part of the Himalaya in central Nepal, has the thickest orogenic core. Moreover, corresponding to the distribution of thickened orogenic core (thickness >28 km), compared with central Nepal, the topographic swath profile of far-western Nepal is characterized by a wider and gentler frontal part (outer wedge) with high relief and a narrower hinterland (inner wedge) with high-elevation, low-relief landscape (Fig. 5). The approximate collocation between the thickened orogenic core (thickness >28 km) and the areas of high-elevation, low-relief (inner wedge) to the north of the uplifting front, regard-

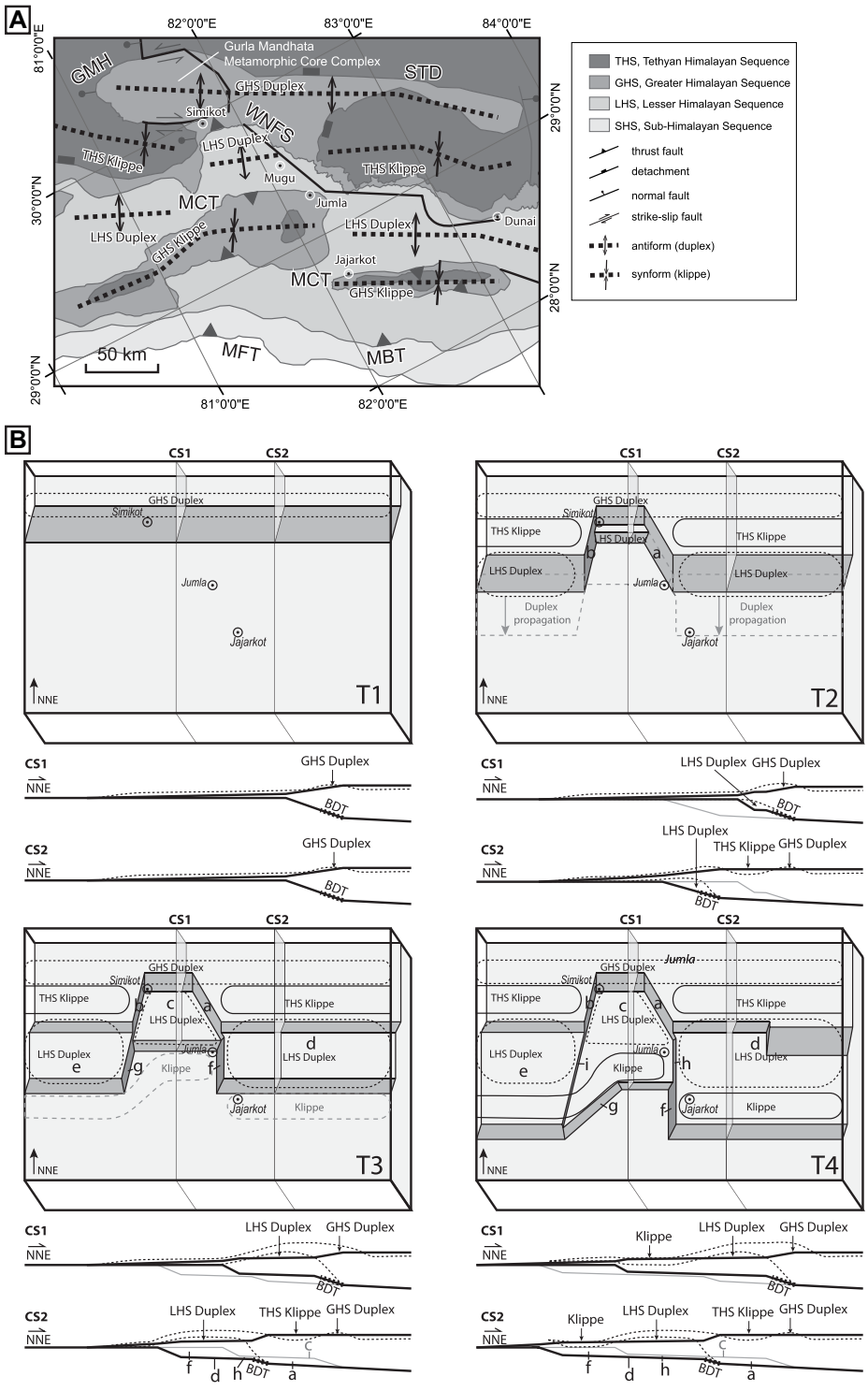

Figure 6. (A) Geologic map of far-western Nepal and adjacent areas. Notice the misalignment of antiformal and synformal features along their strike and the partial collocation between the Western Nepal fault system (WNFS) and transitional positions between the antiformal and synformal features. (B) General evolution of the lateral and oblique ramps (a, b, f, g, h, i) in the Main Himalayan Thrust (MHT) and antiformal and synformal features in schematic block diagrams and cross-sections through time (T1–T4). The c, d, e are flats in the MHT connecting the deeper and higher frontal ramps. In the block diagrams, the dark gray parts represent the ramps in the lower plate of the MHT and the black solid and dash rounded rectangles represent where klippen and duplexes developed, respectively. The gray dashed areas in T2 and T3 represent the structures developing in the next step. In each cross-section, the two black solid lines are the topography (higher) and MHT (lower) at the time, respectively, and the two dash lines are the South Tibet Detachment (STD) (higher) and Main Central Thrust (MCT) (lower), respectively. The solid gray line is the projected MHT from the other cross-section at the time. The space bounded by the two MHTs (black and gray) on each cross-section represents the projection of the lateral ramps (e.g., f, h) between the central and eastern sectors. The abrupt increase in the topography coincides with the brittle-ductile transition zone (BDT, represented with bold dash line) along the mid-lower crustal ramp of the MHT. GMH—Gurla Mandhata-Humla fault system; MBT—Main Boundary Thrust; MFT—Main Frontal Thrust.

less of the along-strike changes in their width (Figs. 4 and 5), suggests that mid-lower crustal duplexing at the brittle-ductile transition zone is an effective mechanism for orogenic plateau growth. The outward growth of the orogenic plateau is accompanied with foreland-ward migration of the mid-lower crustal duplexing.

MHT Ramp Geometry

The apparent along-strike "abnormal" rheology pattern of the MHT in far-western Nepal may reflect an along-strike change in its geometry as noted by several studies (Harvey et al., 2015; Hubbard et al., 2016; van der Beek et al., 2016; Hoste-Colomer et al., 2018; Lindsey et al., 2018; Soucy La Roche and Godin, 2019), which we interpret to be a system of lateral, oblique, and frontal ramps. Assuming the rheology of the MHT is controlled by temperature and the area has uniform geothermal gradient along strike, lateral, or oblique ramps will result in the structurally higher megathrust intersecting the nominal temperature range for ductile strain at a position farther north from that on the lower megathrust. The surface geology also suggests the possible existence of lateral or oblique ramps affecting the foreland-ward propagation of the deformation. At approximately the longitude of the embayment discussed above, the trace of the MCT, LHS duplex, and the long axis of the Almora-Dadeldhura klippe, all shift toward the hinterland (north). This results in the alignment of antiformal features, such as LHS duplexes, and synformal features, such as GHS klippen and THS half-klippen, along their strike (Fig. 6A).

Based on our interpretation of an along-strike heterogeneous MHT rheology, we synthesize the geologic information from the outer wedge and propose a conceptual model for the geometry and evolution of the ramps in the MHT in western Nepal (Fig. 6B). We interpret the ramp positions using criteria as follows: (1) a frontal ramp exists in the mid-lower crust in the hinterland where the brittle-ductile zone lies, and its location is represented by the actively uplifting front on the surface as described earlier; (2) a higher frontal ramp exists where LHS is duplexed or imbricated and evolves via foreland propagation (refer to Robinson et al., 2003 for details); (3) the along-strike transition between the antiformal and synformal features indicates the locations of the higher frontal ramps vary along strike, which requires the lateral or high-angle oblique ramps of the MHT to connect them. In the model (Fig. 6B), at time T1, after the MCT and STD ceased, a single ramp was in the hinterland extending through the crust, mid-lower crust was accreted at the brittle-ductile transition zone along the ramp forming the GHS duplex. The North Himalayan antiform started to develop along the ramp and was the active uplifting front at that time. At T2, to the east and west of the topographic embayment today, the megathrust propagated to the south of where the THS half-klippen are present today and a new ramp formed at this position. At the topographic embayment sector (central sector), the frontal ramp did not change location. Thus, in this step, the North Himalayan antiform continued to grow only in the central sector. In the western and eastern sectors, the North Himalayan antiform stopped growing and the synformal THS half-klippen formed, as ductile duplexing at the brittle-ductile transition zone and the active uplifting front shifted southward to the new ramp. The lateral or oblique ramps (a, b in Fig. 6B) formed and connected the frontal ramps in three sectors. From T2 to T3, the frontal ramp in each sector broke into two ramps connected by a flat (c, d, e in Fig. 6B). In each sector, the new higher frontal ramp and the flat in upper crust propagated toward the foreland via subsequently excising LHS sheets from the footwall and incorporating them as horses into the antiformal LHS duplex in the hanging wall. In the central sector, because no THS klippe formed between the GHS duplex and the LHS duplex, the GHS duplex is juxtaposed against the LHS directly causing the abnormally high STD in the 3-D model (Fig. 2). From T3 to T4, in each sector, the higher frontal ramp shifted farther to the foreland and the synformal GHS klippen formed between the LHS duplexes and the location of the new ramp. From T2 to T4, the antiformal and synformal features in the outer wedge developed as the MHT flats (c, d, e in Fig. 6B) above the mid-lower crustal ramp continuously propagated to the foreland and generated new upper frontal ramps (e.g., DeCelles et al., 2001; Robinson et al., 2003). Structural restoration of three cross-sections suggests that the along-strike transition between the antiformal and synformal features was controlled by the number of LHS horses that have been stacked up and the amount of shortening accommodated by each of them (Robinson et al., 2006). If these variations were not completely accommodated by internal structures, like tear faults, in the hanging wall of the MHT, it requires the existence of the lateral or oblique ramps (f, g) connecting the contemporary higher frontal ramps (Fig. 6B). This type of lateral and oblique ramps also propagated to the foreland correspondently as new frontal ramps formed when new LHS horses got involved in the deformation. If the flats (c, d, e) connecting the deeper and higher frontal ramps in adjacent sectors were of different depths, later ramps (h, i) could be preserved between the flats after the lateral ramps (f, g) connecting the higher frontal ramps propagated to the south (Fig. 6B). Similarly, they could not be preserved if the LHS horses at the three sectors developed on the flats (c, d, e) of the same depth. In the whole process from T1 to T4, the location of the uplifting front always corresponds to the brittle-ductile transition zone along the northern lower frontal ramp, and the orogenic plateau (regions of high-elevation, low-relief) grows outward as this location migrates foreland-ward. The embayment of the actively uplifting front developed at T2 due to the formation of the lateral or oblique ramps of the MHT and its shape did not significantly change since then. The trace of the WNFZ from Simikot to Dunai coincidently follows the features affected by the oblique or lateral ramps, such as the actively uplifting front and the roof thrust of the LHS duplex, suggesting it is the upper crustal expression of the ramps in the MHT (Fig. 6A).

The location and geometry of megathrust ramps are of great significance in seismic hazard assessment because ramps can act as barriers to rupture propagation during large earthquakes. This has been well observed in various studies on the 2015 M_w 7.8 Gorkha earthquake of which the slip patch matches an oval-shaped, gently dipping fault surface bounded on all sides by steeper ramps (Duputel et al., 2016; Elliott et al., 2016; Hubbard et al., 2016; Wang et al., 2017). The eastern and western ends of the aftershock zone of the Gorkha earthquake correspond to seismic wave speed increase at MHT depth (Bai et al., 2019) and to changes in structural pattern at the surface (Grandin et al., 2015), suggesting along-strike change in the megathrust structure. 2-D dip model of the MHT estimated by geodetic data analysis also confirms the lateral change in the dip (Zhang et al., 2017). Although lateral changes in the geometry of the MHT in western Nepal has been proposed and discussed in many studies (e.g., Robert et al., 2011; Harvey et al., 2015; Bollinger et al., 2016; Hubbard et al., 2016; Hoste-Colomer et al., 2018; Subedi et al., 2018; Soucy La Roche and Godin, 2019), its geometry is still not well understood. However, significant seismic hazard exists in the area because large historical earthquakes have been reported (Murphy et al., 2014; Bollinger et al., 2016; Hossler et al., 2016) in the area and the along-strike extent of the region devastated in the 1505 AD earthquake roughly corresponds to the "embayment" in western Nepal discussed earlier, from Thakkola graben to Gurla Mandhata (Bollinger et al., 2016). The earthquakes rupturing the WNFS are approximately coeval with some historical large earthquakes (Murphy et al., 2014), suggesting the important role of the ramp geometry in controlling rupture propagation. The ramps interpreted in this study may explain why the western terminus of the 1505 AD earthquake rupture is located near the Gurla Mandhata area.

CONCLUSIONS

Our 3-D model of the metamorphosed orogenic core of the western and central Himalaya shows significant along-strike variation in the thickness, from ~25–26 km in the western Himalaya to ~34–42 km in the central Himalaya, suggesting significant along-strike strain variation. The abrupt change lies at the western boundary of the Gurla Mandhata MCC, suggesting significant change in the strain state. Assuming the thickness of the orogenic core at 37 Ma was 17 km and constant along the strike, the western and central Himalaya has been thickened by 0.5 and 1–1.5 times, respectively. We propose an oblique convergence model, which describes OP extensional strain partition in the western Himalayan as the driver for the dramatic along-strike strain variation and many associated features, such as metamorphic core complexes, OP stretching lineation and shear zones within the orogenic core and a supradetachment basin with a low subsidence rate. The initiation of the upper crustal strain partitioning could be triggered by increased convergence obliquity in the western Himalaya via rotational shortening and/or oroclinal bending and/or the formation of a weak rear back via the development of the GCT and south propagation of the Karakoram fault in middle-late Miocene. The brittle-ductile transition zone along the megathrust is where strain locally accumulates, and mid-lower crustal duplexing develops. Thus, it correlates to the

uplifting front of the orogenic plateau. The hinterland-ward shift of the brittle-ductile transition zone of the MHT in far-western Nepal caused the continuously focused thickening in a narrow area in the hinterland, generating the thickest part of the orogenic core. The comparison of the model along its strike and with other datasets suggests that mid-lower crustal duplexing at the brittle-ductile transition zone is an effective mechanism of outward growth of a hinterland plateau. The along-strike variation in the location of the brittle-ductile transition zone along the megathrust may be caused by the existence of lateral and oblique ramps as suggested by the surface geology.

ACKNOWLEDGEMENTS

This study was funded by National Science Foundation grant (no. 1827863) to Michael A. Murphy. We acknowledge John Cannon for contributing normalized river channel steepness data. We thank Rodolfo Carosi and two anonymous reviewers for their very careful, critical comments, and constructive suggestions that greatly improved the manuscript. Authors also thank Midland Valley Exploration for providing academic licenses for MOVE software.

REFERENCES CITED

Adams, B.A., Hodges, K.V., van Soest, M.C., and Whipple, K.X., 2013, Evidence for Pliocene–Quaternary normal faulting in the hinterland of the Bhutan Himalaya: Lithosphere, v. 5, no. 4, p. 438–449, https://doi.org/10.1130/L277.1.

Adams, B.A., Whipple, K.X., Hodges, K.V., and Heimsath, A.M., 2016, In situ development of high-elevation, low-relief landscapes via duplex deformation in the Eastern Himalayan hinterland, Bhutan: Journal of Geophysical Research. Earth Surface, v. 121, no. 2, p. 294–319, https://doi.org/10.1002/2015JF003508.

Ader, T., Avouac, J.P., Liu-Zeng, J., Lyon-Caen, H., Bollinger, L., Galetzka, J., Genrich, J., Thomas, M., Chanard, K., Sapkota, S.N., Rajaure, S., Shrestha, P., Ding, L., and Flouzat, M., 2012, Convergence rate across the Nepal Himalaya and interseismic coupling on the Main Himalayan Thrust: Implications for seismic hazard: Journal of Geophysical Research. Solid Earth, v. 117, no. B4, https://doi.org/10.1029/2011JB009071.

Aikman, A.B., Harrison, T.M., and Lin, D., 2008, Evidence for early (>44 Ma) Himalayan crustal thickening, Tethyan Himalaya, southeastern Tibet: Earth and Planetary Science Letters, v. 274, no. 1–2, p. 14–23, https://doi.org/10.1016/j.epsl.2008.06.038.

Arita, K., 1983, Origin of the inverted metamorphism of the lower Himalayas, Central Nepal: Tectonophysics, v. 95, no. 1, p. 43–60, https://doi.org/10.1016/0040-1951(83)90258-5.

Avouac, J.P., and Burov, E.B., 1996, Erosion as a driving mechanism of intracontinental mountain growth: Journal of Geophysical Research. Solid Earth, v. 101, no. B8, p. 17747–17769, https://doi.org/10.1029/96JB01344.

Bai, L., Klemperer, S.L., Mori, J., Karplus, M.S., Ding, L., Liu, H., Li, G., Song, B., and Dhakal, S., 2019, Lateral variation of the Main Himalayan Thrust controls the rupture length of the 2015 Gorkha earthquake in Nepal: Science Advances, v. 5, no. 6, https://doi.org/10.1126/sciadv.aav0723.

Beaumont, C., Jamieson, R.A., Nguyen, M.H., and Lee, B., 2001, Himalayan tectonics explained by extrusion of a low-viscosity crustal channel coupled to focused surface denudation: Nature, v. 414, no. 6865, p. 738–742, https://doi.org/10.1038/414738a.

Bendick, R., and Bilham, R., 2001, How perfect is the Himalayan arc?: Geology, v. 29, no. 9, p. 791–794, https://doi.org/10.1130/0091-7613(2001)029<0791:HPITHA>2.0.CO;2.

Bilham, R., Larson, K., Freymueller, J., Jouanne, F., LeFort, P., Leturmy, P., Mugnier, J.L., Gamond, J.F., Glot, J.P., Martinod, J., Chaudury, N.L., Chitrakar, G.R., Gautam, U.P., Koirala, B.P., Pandey, M.R., Ranabhat, R., Sapkota, S.N., Shrestha, P.L., Thakuri, M.C., Timilsina, U.R., Tiwari, D.R., Vidal, G., Vigny, C., Galy, A., and deVoogd, B., 1997, GPS measurements of present-day convergence across the Nepal Himalaya: Nature, v. 386, no. 6620, p. 61–64, https://doi.org/10.1038/386061a0.

Bollinger, L., Henry, P., and Avouac, J., 2006, Mountain building in the Nepal Himalaya: Thermal and kinematic model: Earth and Planetary Science Letters, v. 244, no. 1–2, p. 58–71, https://doi.org/10.1016/j.epsl.2006.01.045.

Bollinger, L., Tapponnier, P., Sapkota, S.N., and Klinger, Y., 2016, Slip deficit in central Nepal: Omen for a repeat of the 1344 AD earthquake?: Earth, Planets, and Space, v. 68, no. 12, p. 1–12, https://doi.org/10.1186/s40623-016-0389-1.

Braden, Z., Godin, L., Cottle, J., and Yakymchuk, C., 2018, Renewed late Miocene (<8 Ma) hinterland ductile thrusting, western Nepal Himalaya: Geology, v. 46, no. 6, p. 503–506, https://doi.org/10.1130/G40097.1.

Brunel, M., 1986, Ductile thrusting in the Himalayas: Shear sense criteria and stretching lineations: Tectonics, v. 5, no. 2, p. 247–265, https://doi.org/10.1029/TC005i002p00247.

Burbank, D.W., Blythe, A.E., Putkonen, J., Pratt-Sitaula, B., Gabet, E., Oskin, M., Barros, A., and Ojha, T.P., 2003, Decoupling of erosion and precipitation in the Himalayas: Nature, v. 426, no. 6967, p. 652–655, https://doi.org/10.1038/nature02187.

Burchfiel, B.C., Zhiliang, C., Hodges, K.V., Yuping, L., Royden, L.H., Changrong, D., and Jiene, X., 1992, The South Tibetan Detachment System, Himalayan Orogen: Extension Contemporaneous With and Parallel to Shortening in a Collisional Mountain Belt: Geological Society of America Special Papers, v. 269, 41 p., https://doi.org/10.1130/SPE269.

Burg, J.P., and Chen, G.M., 1984, Tectonics and structural zonation of Southern Tibet, China: Nature, v. 311, no. 5983, p. 219–223, https://doi.org/10.1038/311219a0.

Burg, J.P., Brunel, M., Gapais, D., Chen, G.M., and Liu, G.H., 1984, Deformation of leucogranites of the crystalline Main Central Sheet in southern Tibet (China): Journal of Structural Geology, v. 6, no. 5, p. 535–542, https://doi.org/10.1016/0191-8141(84)90063-4.

Butler, R.W.H., 1982a, Hangingwall strain: A function of duplex shape and footwall topography: Tectonophysics, v. 88, no. 3–4, p. 235–246, https://doi.org/10.1016/0040-1951(82)90238-4.

Butler, R.W.H., 1982b, The terminology of structures in thrust belts: Journal of Structural Geology, v. 4, no. 3, p. 239–245, https://doi.org/10.1016/0191-8141(82)90011-6.

Caldwell, W. B., Klemperer, S. L., Lawrence, J. F., Rai, S. S., and Ashish, 2013, Characterizing the Main Himalayan Thrust in the Garhwal Himalaya, India with receiver function CCP stacking: Earth and Planetary Science Letters, v. 367, p. 15–27, https://doi.org/10.1016/j.epsl.2013.02.009.

Cannon, J.M., and Murphy, M.A., 2014, Active lower crustal deformation and Himalayan seismic hazard revealed by stream channels and regional geology: Tectonophysics, v. 633, p. 34–42, https://doi.org/10.1016/j.tecto.2014.06.031.

Cannon, J.M., Murphy, M.A., and Taylor, M., 2018, Segmented strain accumulation in the High Himalaya expressed in river channel steepness: Geosphere, v. 14, no. 3, p. 1131–1149, https://doi.org/10.1130/GES01508.1.

Carosi, R., Lombardo, B., Molli, G., Musumeci, G., and Pertusati, P.C., 1998, The south Tibetan detachment system in the Rongbuk valley, Everest region. Deformation features and geological implications: Journal of Asian Earth Sciences, v. 16, no. 2, p. 299–311, https://doi.org/10.1016/S0743-9547(98)00014-2.

Carosi, R., Montomoli, C., Rubatto, D., and Visonà, D., 2006, Normal-sense shear zones in the core of the Higher Himalayan Crystallines (Bhutan Himalaya): Evidence for extrusion?, *in* Law, R.D., Searle, M.P., and Godin, L., eds., Channel Flow, Ductile Extrusion and Exhumation in Continental Collision Zones: Geological Society of London, Special Publications, v. 268, no. 1, p. 425–444, https://doi.org/10.1144/GSL.SP.2006.268.01.20.

Carosi, R., Montomoli, C., and Visonà, D., 2007, A structural transect in the Lower Dolpo: Insights on the tectonic evolution of Western Nepal: Journal of Asian Earth Sciences, v. 29, no. 2–3, p. 407–423, https://doi.org/10.1016/j.jseaes.2006.05.001.

Carosi, R., Montomoli, C., Rubatto, D., and Visona, D., 2013, Leucogranite intruding the South Tibetan Detachment in western Nepal: Implications for exhumation models in the Himalayas: Terra Nova, v. 25, no. 6, p. 478–489, https://doi.org/10.1111/ter.12062.

Carosi, R., Montomoli, C., Langone, A., Turina, A., Cesare, B., Iaccarino, S., Fascioli, L., Visonà, D., Ronchi, A., and Rai, S.M., 2015, Eocene partial melting recorded in peritectic garnets from kyanite-gneiss, Greater Himalayan Sequence, central Nepal, *in* Mukherjee, S., Carosi, R., van der Beek, P.A., Mukherjee, B.K., and Robinson, D.M., eds., Tectonics of the Himalaya: Geological Society of London, Special Publications, v. 412, no. 1, p. 111–129, https://doi.org/10.1144/SP412.1.

Carosi, R., Montomoli, C., Iaccarino, S., Massonne, H.J., Rubatto, D., Langone, A., Gemignani, L., and Visona, D., 2016, Middle to late Eocene exhumation of the Greater Himalayan Sequence in the Central Himalayas: Progressive accretion from the Indian plate: Geological Society of America Bulletin, v. 128, no. 11–12, p. 1571–1592, https://doi.org/10.1130/B31471.1.

Carosi, R., Montomoli, C., and Iaccarino, S., 2018, 20 years of geological mapping of the metamorphic core across Central and Eastern Himalayas: Earth-Science Reviews, v. 177, p. 124–138, https://doi.org/10.1016/j.earscirev.2017.11.006.

Catlos, E.J., Harrison, T.M., Kohn, M.J., Grove, M., Ryerson, F.J., Manning, C.E., and Upreti, B.N., 2001, Geochronologic and thermobarometric constraints on the evolution of the Main Central Thrust, central Nepal Himalaya: Journal of Geophysical Research. Solid Earth, v. 106, no. B8, p. 16177–16204, https://doi.org/10.1029/2000JB900375.

Catlos, E.J., Harrison, T.M., Manning, C.E., Grove, M., Rai, S.M., Hubbard, M.S., and Upreti, B.N., 2002, Records of the evolution of the Himalayan orogen from in situ Th-Pb ion microprobe dating of monazite: Eastern Nepal and western Garhwal: Journal of Asian Earth Sciences, v. 20, no. 5, p. 459–479, https://doi.org/10.1016/S1367-9120(01)00039-6.

Cattin, R., and Avouac, J.P., 2000, Modeling mountain building and the seismic cycle in the Himalaya of Nepal: Journal of Geophysical Research. Solid Earth, v. 105, no. B6, p. 13389–13407, https://doi.org/10.1029/2000JB900032.

Célérier, J., Harrison, T.M., Beyssac, O., Herman, F., Dunlap, W.J., and Webb, A.A.G., 2009, The Kumaun and Garwhal Lesser Himalaya, India: Part 2. Thermal and deformation histories: Geological Society of America Bulletin, v. 121, no. 9–10, p. 1281–1297, https://doi.org/10.1130/B26343.1.

Clerc, C., Jolivet, L., and Ringenbach, J.C., 2015, Ductile extensional shear zones in the lower crust of a passive margin: Earth and Planetary Science Letters, v. 431, p. 1–7, https://doi.org/10.1016/j.epsl.2015.08.038.

Coleman, M.E., 1996, Orogen-parallel and orogen-perpendicular extension in the central Nepalese Himalayas: Geological Society of America Bulletin, v. 108, no. 12, p. 1594–1607, https://doi.org/10.1130/0016-7606(1996)108<1594:OPAOPE>2.3.CO;2.

Coleman, M., and Hodges, K., 1995, Evidence for Tibetan plateau uplift before 14 Myr ago from a new minimum age for east–west extension: Nature, v. 374, no. 6517, p. 49–52, https://doi.org/10.1038/374049a0.

Coleman, M.E., and Hodges, K.V., 1998, Contrasting Oligocene and Miocene thermal histories from the hanging wall and footwall of the South Tibetan detachment in the central Himalaya from $^{40}Ar/^{39}Ar$ thermochronology, Marsyandi Valley, central Nepal: Tectonics, v. 17, no. 5, p. 726–740, https://doi.org/10.1029/98TC02777.

Cooper, F.J., Hodges, K.V., and Adams, B.A., 2013, Metamorphic constraints on the character and displacement of the South Tibetan fault system, central Bhutanese Himalaya: Lithosphere, v. 5, no. 1, p. 67–81, https://doi.org/10.1130/L221.1.

Cottle, J.M., Waters, D.J., Riley, D., Beyssac, O., and Jessup, M.J., 2011, Metamorphic history of the South Tibetan Detachment System, Mt. Everest region, revealed by RSCM thermometry and phase equilibria modelling: Journal of Metamorphic Geology, v. 29, no. 5, p. 561–582, https://doi.org/10.1111/j.1525-1314.2011.00930.x.

Cottle, J.M., Larson, K.P., and Kellett, D.A., 2015a, How does the mid-crust accommodate deformation in large, hot collisional orogens? A review of recent research in the Himalayan orogen: Journal of Structural Geology, v. 78, p. 119–133, https://doi.org/10.1016/j.jsg.2015.06.008.

Cottle, J.M., Searle, M.P., Jessup, M.J., Crowley, J.L., and Law, R.D., 2015b, Rongbuk re-visited: Geochronology of leucogranites in the footwall of the South Tibetan Detachment System, Everest Region, Southern Tibet: Lithos, v. 227, p. 94–106, https://doi.org/10.1016/j.lithos.2015.03.019.

Coutand, I., Whipp, D.M., Grujic, D., Bernet, M., Fellin, M.G., Bookhagen, B., Landry, K.R., Ghalley, S.K., and Duncan, C., 2014, Geometry and kinematics of the Main Himalayan Thrust and Neogene crustal exhumation in the Bhutanese Himalaya derived from inversion of multithermochronologic data: Journal of Geophysical Research. Solid Earth, v. 119, no. 2, p. 1446–1481, https://doi.org/10.1002/2013JB010891.

Crouzet, C., Gautam, P., Schill, E., and Appel, E., 2003, Multicomponent magnetization in western Dolpo (Tethyan Himalaya, Nepal): Tectonic implications: Tectonophysics, v. 377, no. 1–2, p. 179–196, https://doi.org/10.1016/j.tecto.2003.08.019.

DeCelles, P.G., Gehrels, G.E., Quade, J., and Ojha, T.P., 1998, Eocene-early Miocene foreland basin development and the history of Himalayan thrusting, western and central Nepal: Tectonics, v. 17, no. 5, p. 741–765, https://doi.org/10.1029/98TC02598.

DeCelles, P.G., Robinson, D.M., Quade, J., Ojha, T.P., Garzione, C.N., Copeland, P., and Upreti, B.N., 2001, Stratigraphy, structure, and tectonic evolution of the Himalayan fold-thrust belt in western Nepal: Tectonics, v. 20, no. 4, p. 487–509, https://doi.org/10.1029/2000TC001226.

DeCelles, P.G., Kapp, P., Quade, J., and Gehrels, G.E., 2011, Oligocene–Miocene Kailas basin, southwestern Tibet: Record of postcollisional upper-plate extension in the Indus-Yarlung suture zone: Geological Society of America Bulletin, v. 123, no. 7–8, p. 1337–1362, https://doi.org/10.1130/B30258.1.

Ding, L., Kapp, P., and Wan, X., 2005, Paleocene-Eocene record of ophiolite obduction and initial India-Asia collision, south central Tibet: Tectonics, v. 24, no. 3, https://doi.org/10.1029/2004TC001729.

Dunkl, I., Antolín, B., Wemmer, K., Rantitsch, G., Kienast, M., Montomoli, C., Ding, L., Carosi, R., Appel, E., El Bay, R., Xu, Q., and Von Eynatten, H., 2011, Metamorphic evolution of the Tethyan Himalayan flysch in SE Tibet, *in* Gloaguan, R., and Ratschbacher, L., eds., Growth and Collapse of the Tibetan Plateau: Geological Society of London, Special Publications, v. 353, no. 1, p. 45–69, https://doi.org/10.1144/SP353.4.

Duputel, Z., Vergne, J., Rivera, L., Wittlinger, G., Farra, V., and Hetényi, G., 2016, The 2015 Gorkha earthquake: A large event illuminating the Main Himalayan Thrust fault: Geophysical Research Letters, v. 43, no. 6, p. 2517–2525, https://doi.org/10.1002/2016GL068083.

Edwards, M.A., Kidd, W.S.F., Li, J., Yue, Y., and Clark, M., 1996, Multi-stage development of the southern Tibet detachment system near Khula Kangri: New data from Gonto La: Tectonophysics, v. 260, no. 1, p. 1–19, https://doi.org/10.1016/0040-1951(96)00073-X.

Eizenhöfer, P.R., McQuarrie, N., Shelef, E., and Ehlers, T.A., 2019, Landscape response to lateral advection in convergent orogens over geologic time scales: Journal of Geophysical Research. Earth Surface, v. 124, no. 8, p. 2056–2078, https://doi.org/10.1029/2019JF005100.

Elliott, J.R., Jolivet, R., González, P.J., Avouac, J.P., Hollingsworth, J., Searle, M.P., and Stevens, V.L., 2016, Himalayan megathrust geometry and relation to topography revealed by the Gorkha earthquake: Nature Geoscience, v. 9, no. 2, p. 174–180, https://doi.org/10.1038/ngeo2623 (corrigendum: https://doi.org/10.1038/ngeo2810).

Flórez-Rodríguez, A.G., Schellart, W.P., and Strak, V., 2019, Impact of aseismic ridges on subduction systems: Insights from analog modeling: Journal of Geophysical Research. Solid Earth, v. 124, no. 6, p. 5951–5969, https://doi.org/10.1029/2019JB017488.

Friedmann, S.J., and Burbank, D.W., 1995, Rift basins and supradetachment basins: intracontinental extensional end-members: Basin Research, v. 7, no. 2, p. 109–127, https://doi.org/10.1111/j.1365-2117.1995.tb00099.x.

Fuller, C.W., Willett, S.D., and Brandon, M.T., 2006, Formation of forearc basins and their influence on subduction zone earthquakes: Geology, v. 34, no. 2, p. 65–68, https://doi.org/10.1130/G21828.1.

Gaetani, M., and Garzanti, E., 1991, Multicyclic history of the northern India continental margin (Northwestern Himalaya) (1): AAPG Bulletin, v. 75, no. 9, p. 1427–1446.

Gansser, A., 1964, Geology of the Himalayas: London, UK, John Wiley and Sons Ltd, 308 p.

Gao, R., Lu, Z., Klemperer, S.L., Wang, H., Dong, S., Li, W., and Li, H., 2016, Crustal-scale duplexing beneath the Yarlung Zangbo suture in the western Himalaya: Nature Geoscience, v. 9, no. 7, p. 555–560, https://doi.org/10.1038/ngeo2730.

Garzione, C.N., DeCelles, P.G., Hodkinson, D.G., Ojha, T.P., and Upreti, B.N., 2003, East-west extension and Miocene environmental change in the southern Tibetan plateau: Thakkhola graben, central Nepal: Geological Society of America Bulletin, v. 115, no. 1, p. 3–20, https://doi.org/10.1130/0016-7606(2003)115<0003:EWEAME>2.0.CO;2.

Godin, L., Brown, R.L., and Hanmer, S., 1999, High strain zone in the hanging wall of the Annapurna detachment, central Nepal Himalaya, *in* Macfarlane, A., Sorkhabi, R.B., and Quade, J., eds., Himalaya and Tibet: Mountain Roots to Mountain Tops: Geological Society of America Special Papers, v. 328, p. 199–210, https://doi.org/10.1130/0-8137-2328-0.199.

Godin, L., Gleeson, T.P., Searle, M.P., Ullrich, T.D., and Parrish, R.R., 2006, Locking of southward extrusion in favour of rapid crustal-scale buckling of the Greater Himalayan sequence, Nar valley, central Nepal: Channel Flow: Ductile Extrusion and Exhumation in Continental Collision Zones, v. 268, no. 1, p. 269–292, https://doi.org/10.1144/GSL.SP.2006.268.01.13.

Grandin, R., Vallée, M., Satriano, C., Lacassin, R., Klinger, Y., Simoes, M., and Bollinger, L., 2015, Rupture process of the Mw = 7.9 2015 Gorkha earthquake (Nepal): Insights into Himalayan megathrust segmentation: Geophysical Research Letters, v. 42, no. 20, p. 8373–8382, https://doi.org/10.1002/2015GL066044.

Guo, X., Li, W., Gao, R., Xu, X., Li, H., Huang, X., Ye, Z., Lu, Z., and Klemperer, S.L., 2017, Nonuniform subduction of the Indian crust beneath the Himalayas: Scientific Reports, v. 7, no. 12497, https://doi.org/10.1038/s41598-017-12908-0.

Guo, X., Gao, R., Zhao, J., Xu, X., Lu, Z., Klemperer, S.L., and Liu, H., 2018, Deep-seated lithospheric geometry in revealing collapse of the Tibetan Plateau: Earth-Science Reviews, v. 185, p. 751–762, https://doi.org/10.1016/j.earscirev.2018.07.013.

Hajnal, Z., Lucas, S., White, D., Lewry, J., Bezdan, S., Stauffer, M.R., and Thomas, M.D., 1996, Seismic reflection images of high-angle faults and linked detachments in the Trans-Hudson Orogen: Tectonics, v. 15, no. 2, p. 427–439, https://doi.org/10.1029/95TC02710.

Harvey, J.E., Burbank, D.W., and Bookhagen, B., 2015, Along-strike changes in Himalayan thrust geometry: Topographic and tectonic discontinuities in western Nepal: Lithosphere, v. 7, no. 5, p. 511–518, https://doi.org/10.1130/L444.1.

Heim, A., and Gansser, A., 1939: Geological observations of the Swiss expedition: Denkschriften der Schweizerische Naturforschende Gesellschaft, v. 73, p. 245.

Herman, F., Copeland, P., Avouac, J.P., Bollinger, L., Maheo, G., Le Fort, P., Rai, S., Foster, D., Pecher, A., Stuwe, K., and Henry, P., 2010, Exhumation, crustal deformation, and thermal structure of the Nepal Himalaya derived from the inversion of thermochronological and thermobarometric data and modeling of the topography: Journal of Geophysical Research. Solid Earth, v. 115, no. B6, https://doi.org/10.1029/2008jb006126.

Hintersberger, E., Thiede, R.C., Strecker, M.R., and Hacker, B.R., 2010, East-west extension in the NW Indian Himalaya: Geological Society of America Bulletin, v. 122, no. 9–10, p. 1499–1515, https://doi.org/10.1130/B26589.1.

Hodges, K.V., and Silverberg, D.S., 1988, Thermal evolution of the Greater Himalaya, Garhwal, India: Tectonics, v. 7, no. 3, p. 583–600, https://doi.org/10.1029/TC007i003p00583.

Hodges, K.V., Parrish, R.R., Housh, T.B., Lux, D.R., Burchfiel, B.C., Royden, L.H., and Chen, Z., 1992, Simultaneous Miocene Extension and Shortening in the Himalayan Orogen: Science, v. 258, no. 5087, p. 1466–1470, https://doi.org/10.1126/science.258.5087.1466.

Hodges, K.V., Parrish, R.R., and Searle, M.P., 1996, Tectonic evolution of the central Annapurna Range, Nepalese Himalayas: Tectonics, v. 15, no. 6, p. 1264–1291, https://doi.org/10.1029/96TC01791.

Hopkinson, T., Harris, N., Roberts, N.M.W., Warren, C.J., Hammond, S., Spencer, C.J., and Parrish, R.R., 2019, Evolution of the melt source during protracted crustal anatexis: An example from the Bhutan Himalaya: Geology, v. 48, p. 87–91, https://doi.org/10.1130/g47078.1.

Hossler, T., Bollinger, L., Sapkota, S.N., Lavé, J., Gupta, R.M., and Kandel, T.P., 2016, Surface ruptures of large Himalayan earthquakes in Western Nepal: Evidence along a reactivated strand of the Main Boundary Thrust: Earth and Planetary Science Letters, v. 434, p. 187–196, https://doi.org/10.1016/j.epsl.2015.11.042.

Hoste-Colomer, R., Bollinger, L., Lyon-Caen, H., Adhikari, L.B., Baillard, C., Benoit, A., Bhattarai, M., Gupta, R.M., Jacques, E., Kandel, T., Koirala, B.P., Letort, J., Maharjan, K., Matrau, R., Pandey, R., and Timsina, C., 2018, Lateral variations of the midcrustal seismicity in western Nepal: Seismotectonic implications: Earth and Planetary Science Letters, v. 504, p. 115–125, https://doi.org/10.1016/j.epsl.2018.09.041.

Hubbard, J., Almeida, R., Foster, A., Sapkota, S.N., Bürgi, P., and Tapponnier, P., 2016, Structural segmentation controlled the 2015 M_w 7.8 Gorkha earthquake rupture in Nepal: Geology, v. 44, no. 8, p. 639–642, https://doi.org/10.1130/G38077.1.

Huntington, K.W., Saylor, J., Quade, J., and Hudson, A.M., 2015, High late Miocene–Pliocene elevation of the Zhada Basin, southwestern Tibetan Plateau, from carbonate clumped isotope thermometry: Geological Society of America Bulletin, v. 127, no. 1–2, p. 181–199, https://doi.org/10.1130/B31000.1.

Hyndman, R.D., Yamano, M., and Oleskevich, D.A., 1997, The seismogenic zone of subduction thrust faults: The Island Arc, v. 6, no. 3, p. 244–260, https://doi.org/10.1111/j.1440-1738.1997.tb00175.x.

Iaccarino, S., Montomoli, C., Carosi, R., Massonne, H.J., Langone, A., and Visona, D., 2015, Pressure-temperature-time-deformation path of kyanite-bearing migmatitic paragneiss in the Kali Gandaki valley (Central Nepal): Investigation of Late Eocene-Early Oligocene melting processes: Lithos, v. 231, p. 103–121, https://doi.org/10.1016/j.lithos.2015.06.005.

Iaccarino, S., Montomoli, C., Carosi, R., Massonne, H.J., and Visona, D., 2017, Geology and tectono-metamorphic evolution of the Himalayan metamorphic core: Insights from the Mugu Karnali transect, Western Nepal (Central Himalaya): Journal of Metamorphic Geology, v. 35, no. 3, p. 301–325, https://doi.org/10.1111/jmg.12233.

Inger, S., and Harris, N.B.W., 1992, Tectonothermal evolution of the High Himalayan Crystalline Sequence, Langtang Valley, northern Nepal: Journal of Metamorphic Geology, v. 10, no. 3, p. 439–452, https://doi.org/10.1111/j.1525-1314.1992.tb00095.x.

Jessup, M.J., Law, R.D., Searle, M.P., and Hubbard, M.S., 2006, Structural evolution and vorticity of flow during extrusion and exhumation of the Greater Himalayan Slab, Mount Everest Massif, Tibet/Nepal: Implications for orogen-scale flow partitioning, *in* Law, R.D., Searle, M.P., and Godin, L., eds., Channel Flow, Ductile Extension and Exhumation in Continental Collision Zones: Geological Society of London, Special Publications, v. 268, no. 1, p. 379–413, https://doi.org/10.1144/GSL.SP.2006.268.01.18.

Jessup, M.J., Newell, D.L., Cottle, J.M., Berger, A.L., and Spotila, J.A., 2008, Orogen-parallel extension and exhumation enhanced by denudation in the trans-Himalayan Arun River gorge, Ama Drime Massif, Tibet-Nepal: Geology, v. 36, no. 7, p. 587–590, https://doi.org/10.1130/G24722A.1.

Jessup, M.J., Langille, J.M., Diedesch, T.F., and Cottle, J.M., 2019, Gneiss Dome Formation in the Himalaya and southern Tibet, *in* Treloar, P.J., and Searle, M.P., eds., Himalayan Tectonics: A Modern Synthesis: Geological Society of London, Special Publications, v. 483, p. 401–422, https://doi.org/10.1144/SP483.15.

Jolivet, L., Beyssac, O., Goffé, B., Avigad, D., Lepvrier, C., Maluski, H., and Thang, T.T., 2001, Oligo-Miocene midcrustal subhorizontal shear zone in Indochina: Tectonics, v. 20, no. 1, p. 46–57, https://doi.org/10.1029/2000TC900021.

Jolivet, L., Famin, V., Mehl, C., Parra, T., Aubourg, C., Hébert, R., and Philippot, P., 2004, Strain localization during crustal-scale boudinage to form extensional metamorphic domes in the Aegean Sea, *in* Whitney, D., Teyssier, C., and Siddoway, C.S., eds., Gneiss Domes in Orogeny: Geological Society of America Special Papers, v. 380, p. 185–210, https://doi.org/10.1130/0-8137-2380-9.185.

Jones, A.G., Kurtz, R.D., Boerner, D.E., Craven, J.A., McNeice, G.W., Gough, D.I., DeLaurier, J.M., and Ellis, R.G., 1992, Electromagnetic constraints on strike-slip fault geometry: The Fraser River fault system: Geology, v. 20, no. 6, p. 561–564, https://doi.org/10.1130/0091-7613(1992)020<0561:ECOSSF>2.3.CO;2.

Kellett, D.A., and Grujic, D., 2012, New insight into the South Tibetan detachment system: Not a single progressive deformation: Tectonics, v. 31, no. 2, https://doi.org/10.1029/2011tc002957.

Kellett, D.A., Grujic, D., Warren, C., Cottle, J., Jamieson, R., and Tenzin, T., 2010, Metamorphic history of a synconvergent orogen-parallel detachment: The South Tibetan detachment system, Bhutan Himalaya: Journal of Metamorphic Geology, v. 28, no. 8, p. 785–808, https://doi.org/10.1111/j.1525-1314.2010.00893.x.

Kirby, E., and Whipple, K., 2001, Quantifying differential rock-uplift rates via stream profile analysis: Geology, v. 29, no. 5, p. 415–418, https://doi.org/10.1130/0091-7613(2001)029<0415:QDRURV>2.0.CO;2.

Klemperer, S. L., Kennedy, B. M., Sastry, S. R., Makovsky, Y., Harinarayana, T., and Leech, M. L., 2013, Mantle fluids in the Karakoram fault: Helium isotope evidence: Earth and Planetary Science Letters, v. 366, p. 59–70, https://doi.org/10.1016/j.epsl.2013.01.013.

Klootwijk, C.T., Conaghan, P.J., and Powell, C.M., 1985, The Himalayan Arc: Large-scale continental subduction, oroclinal bending and back-arc spreading: Earth and Planetary Science Letters, v. 75, no. 2, p. 167–183, https://doi.org/10.1016/0012-821X(85)90099-8.

Klotz, J., Khazaradze, G., Angermann, D., Reigber, C., Perdomo, R., and Cifuentes, O., 2001, Earthquake cycle dominates contemporary crustal deformation in Central and Southern Andes: Earth and Planetary Science Letters, v. 193, no. 3, p. 437–446, https://doi.org/10.1016/S0012-821X(01)00532-5.

Kohn, M.J., 2014, Himalayan metamorphism and its tectonic implications: Annual Review of Earth and Planetary Sciences, v. 42, no. 1, p. 381–419, https://doi.org/10.1146/annurev-earth-060313-055005.

Kohn, M.J., Wieland, M.S., Parkinson, C.D., and Upreti, B.N., 2005, Five generations of monazite in Langtang gneisses: Implications for chronology of the Himalayan metamorphic core: Journal of Metamorphic Geology, v. 23, no. 5, p. 399–406, https://doi.org/10.1111/j.1525-1314.2005.00584.x.

Kundu, B., Yadav, R.K., Bali, B.S., Chowdhury, S., and Gahalaut, V.K., 2014, Oblique convergence and slip partitioning in the NW Himalaya: Implications from GPS measurements: Tectonics, v. 33, no. 10, p. 2013–2024, https://doi.org/10.1002/2014TC003633.

Landry, K.R., Coutand, I., Whipp, D.M., Grujic, D., and Hourigan, J.K., 2016, Late Neogene tectonically driven crustal exhumation of the Sikkim Himalaya: Insights from inversion of multithermochronologic data: Tectonics, v. 35, no. 3, p. 833–859, https://doi.org/10.1002/2015TC004102.

Langille, J., Lee, J., Hacker, B., and Seward, G., 2010a, Middle crustal ductile deformation patterns in southern Tibet: Insights from vorticity studies in Mabja Dome: Journal of Structural Geology, v. 32, no. 1, p. 70–85, https://doi.org/10.1016/j.jsg.2009.08.009.

Langille, J.M., Jessup, M.J., Cottle, J.M., Newell, D., and Seward, G., 2010b, Kinematic evolution of the Ama Drime detachment: Insights into orogen-parallel extension and exhumation of the Ama Drime Massif, Tibet–Nepal: Journal of Structural Geology, v. 32, no. 7, p. 900–919, https://doi.org/10.1016/j.jsg.2010.04.005.

Langille, J.M., Jessup, M.J., Cottle, J.M., Lederer, G., and Ahmad, T., 2012, Timing of metamorphism, melting and exhumation of the Leo Pargil dome, northwest India: Journal of Metamorphic Geology, v. 30, no. 8, p. 769–791, https://doi.org/10.1111/j.1525-1314.2012.00998.x.

Langille, J.M., Jessup, M.J., Cottle, J., and Ahmad, T., 2014, Kinematic and thermal studies of the Leo Pargil Dome: Implications for synconvergent extension in the NW Indian Himalaya: Tectonics, v. 33, no. 9, p. 1766–1786, https://doi.org/10.1002/2014TC003593.

Larson, K.P., and Godin, L., 2009, Kinematics of the Greater Himalayan sequence, Dhaulagiri Himal: Implications for the structural framework of central Nepal: Journal of the Geological Society, v. 166, no. 1, p. 25–43, https://doi.org/10.1144/0016-76492007-180.

Larson, K.P., Godin, L., Davis, W.J., and Davis, D.W., 2010, Out-of-sequence deformation and expansion of the Himalayan orogenic wedge: insight from the Changgo culmination, south central Tibet: Tectonics, v. 29, no. 4, https://doi.org/10.1029/2008TC002393.

Larson, K.P., Ambrose, T.K., Webb, A.A.G., Cottle, J.M., and Shrestha, S., 2015, Reconciling Himalayan midcrustal discontinuities: The Main Central thrust system: Earth and Planetary Science Letters, v. 429, p. 139–146, https://doi.org/10.1016/j.epsl.2015.07.070.

Laskowski, A.K., Kapp, P., and Cai, F., 2018, Gangdese culmination model: Oligocene–Miocene duplexing along the India-Asia suture zone, Lazi region, southern Tibet: Geological Society of America Bulletin, v. 130, no. 7–8, p. 1355–1376, https://doi.org/10.1130/B31834.1.

Lavé, J., and Avouac, J.P., 2000, Active folding of fluvial terraces across the Siwaliks Hills, Himalayas of central Nepal: Journal of Geophysical Research. Solid Earth, v. 105, no. B3, p. 5735–5770, https://doi.org/10.1029/1999JB900292.

Lavé, J., and Avouac, J.P., 2001, Fluvial incision and tectonic uplift across the Himalayas of central Nepal: Journal of Geophysical Research. Solid Earth, v. 106, no. B11, p. 26561–26591, https://doi.org/10.1029/2001JB000359.

Lavier, L.L., and Manatschal, G., 2006, A mechanism to thin the continental lithosphere at magma-poor margins: Nature, v. 440, p. 324, https://doi.org/10.1038/nature04608.

Law, R.D., Searle, M.P., and Simpson, R.L., 2004, Strain, deformation temperatures and vorticity of flow at the top of the Greater Himalayan Slab, Everest Massif, Tibet: Journal of the Geological Society, v. 161, no. 2, p. 305–320, https://doi.org/10.1144/0016-764903-047.

Law, R.D., Jessup, M.J., Searle, M.P., Francsis, M.K., Waters, D.J., and Cottle, J.M., 2011, Telescoping of isotherms beneath the South Tibetan Detachment System, Mount Everest Massif: Journal of Structural Geology, v. 33, no. 11, p. 1569–1594, https://doi.org/10.1016/j.jsg.2011.09.004.

Law, R.D., Stahr Iii, D.W., Francsis, M.K., Ashley, K.T., Grasemann, B., and Ahmad, T., 2013, Deformation temperatures and flow vorticities near the base of the Greater Himalayan Series, Sutlej Valley and Shimla Klippe, NW India: Journal of Structural Geology, v. 54, p. 21–53, https://doi.org/10.1016/j.jsg.2013.05.009.

Lee, J., and Whitehouse, M.J., 2007, Onset of mid-crustal extensional flow in southern Tibet: Evidence from U/Pb zircon ages: Geology, v. 35, no. 1, p. 45–48, https://doi.org/10.1130/G22842A.1.

Lee, J., Hacker, B.R., Dinklage, W.S., Wang, Y., Gans, P., Calvert, A., Wan, J., Chen, W., Blythe, A.E., and McClelland, W., 2000, Evolution of the Kangmar Dome, southern Tibet: Structural, petrologic, and thermochronologic constraints: Tectonics, v. 19, no. 5, p. 872–895, https://doi.org/10.1029/1999TC001147.

Lee, J., Hacker, B., and Wang, Y., 2004, Evolution of North Himalayan gneiss domes: Structural and metamorphic studies in Mabja Dome, southern Tibet: Journal of Structural Geology, v. 26, no. 12, p. 2297–2316, https://doi.org/10.1016/j.jsg.2004.02.013.

Leech, M.L., 2008, Does the Karakoram fault interrupt midcrustal channel flow in the western Himalaya?: Earth and Planetary Science Letters, v. 276, no. 3, p. 314–322, https://doi.org/10.1016/j.epsl.2008.10.006.

Le Fort, P., 1975, Himalayas: The collided range. Present knowledge of the continental arc: American Journal of Science, v. 275, no. 1, p. 1–44.

Lemiszki, P.J., and Brown, L.D., 1988, Variable crustal structure of strike-slip fault zones as observed on deep seismic reflection profiles: Geological Society of America Bulletin, v. 100, no. 5, p. 665–676, https://doi.org/10.1130/0016-7606(1988)100<0665:VCSOSS>2.3.CO;2.

Lindsey, E.O., Almeida, R., Mallick, R., Hubbard, J., Bradley, K., Tsang, L.L.H., Liu, Y., Burgmann, R., and Hill, E.M., 2018, Structural control on downdip locking extent of the Himalayan megathrust: Journal of Geophysical Research. Solid Earth, v. 123, no. 6, p. 5265–5278, https://doi.org/10.1029/2018JB015868.

Liu, G., and Einsele, G., 1994, Sedimentary history of the Tethyan basin in the Tibetan Himalayas: Geologische Rundschau, v. 83, no. 1, p. 32–61, https://doi.org/10.1007/BF00211893.

Long, S.P., Mullady, C.L., Starnes, J.K., Gordon, S.M., Larson, K.P., Pianowski, L.S., Miller, R.B., and Soignard, E., 2019, A structural model for the South Tibetan detachment system in northwestern Bhutan from integration of temperature, fabric, strain, and kinematic data: Lithosphere, v. 11, no. 4, p. 465–487, https://doi.org/10.1130/L1049.1.

Malatesta, L.C., Bruhat, L., and Finnegan, N.J., 2018, Colocation of the downdip end of seismic locking and the continental shelf break: American Geophysical Union, https://doi.org/10.31223/osf.io/uwzbr.

Martin, A.J., Ganguly, J., and DeCelles, P.G., 2010, Metamorphism of Greater and Lesser Himalayan rocks exposed in the Modi Khola valley, central Nepal: Contributions to Mineralogy and Petrology, v. 159, no. 2, p. 203–223, https://doi.org/10.1007/s00410-009-0424-3.

McCaffrey, R., 1992, Oblique plate convergence, slip vectors, and forearc deformation: Journal of Geophysical Research. Solid Earth, v. 97, no. B6, p. 8905–8915, https://doi.org/10.1029/92JB00483.

McCaffrey, R., and Nabelek, J., 1998, Role of oblique convergence in the active deformation of the Himalayas and southern Tibet plateau: Geology, v. 26, no. 8, p. 691–694, https://doi.org/10.1130/0091-7613(1998)026<0691:ROOCIT>2.3.CO;2.

McCallister, A.T., Taylor, M.H., Murphy, M.A., Styron, R.H., and Stockli, D.F., 2014, Thermochronologic constraints on the late Cenozoic exhumation history of the Gurla Mandhata metamorphic core complex, Southwestern Tibet: Tectonics, v. 33, no. 2, p. 27–52, https://doi.org/10.1002/2013TC003302.

McQuarrie, N., Robinson, D., Long, S., Tobgay, T., Grujic, D., Gehrels, G., and Ducea, M., 2008, Preliminary stratigraphic and structural architecture of Bhutan: Implications for the along strike architecture of the Himalayan system: Earth and Planetary Science Letters, v. 272, no. 1–2, p. 105–117, https://doi.org/10.1016/j.epsl.2008.04.030.

Meigs, A.J., Burbank, D.W., and Beck, R.A., 1995, Middle-late Miocene (>10 Ma) formation of the Main Boundary thrust in the western Himalaya: Geology, v. 23, no. 5, p. 423–426, https://doi.org/10.1130/0091-7613(1995)023<0423:MLMMFO>2.3.CO;2.

Mencin, D., Bendick, R., Upreti, B.N., Adhikari, D.P., Gajurel, A.P., Bhattarai, R.R., Shrestha, H.R., Bhattarai, T.N., Manandhar, N., Galetzka, J., Knappe, E., Pratt-Sitaula, B., Aoudia, A., and Bilham, R., 2016, Himalayan strain reservoir inferred from limited afterslip following the Gorkha earthquake: Nature Geoscience, v. 9, no. 7, p. 533–537, https://doi.org/10.1038/ngeo2734.

Mendoza, M.M., Ghosh, A., Karplus, M.S., Klemperer, S.L., Sapkota, S.N., Adhikari, L.B., and Velasco, A., 2019, Duplex in the Main Himalayan Thrust illuminated by aftershocks of the 2015 M_w 7.8 Gorkha earthquake: Nature Geoscience, v. 12, p. 1018–1022, https://doi.org/10.1038/s41561-019-0474-8.

Montemagni, C., Montomoli, C., Iaccarino, S., Carosi, R., Jain, A.K., Massonne, H.J., and Villa, I.M., 2019, Dating protracted fault activities: Microstructures, microchemistry and geochronology of the Vaikrita Thrust, Main Central Thrust zone, Garhwal Himalaya, NW India, *in* Sharma, R., Villa, I.M., and Kumar, S., eds.,

Crustal Architecture and Evolution of the Himalaya–Karakoram–Tibet Orogen: Geological Society of London, Special Publications, v. 481, no. 1, p. 127–146, https://doi.org/10.1144/SP481.3.

Montomoli, C., Iaccarino, S., Carosi, R., Langone, A., and Visona, D., 2013, Tectonometamorphic discontinuities within the Greater Himalayan Sequence in Western Nepal (Central Himalaya): Insights on the exhumation of crystalline rocks: Tectonophysics, v. 608, p. 1349–1370, https://doi.org/10.1016/j.tecto.2013.06.006.

Montomoli, C., Carosi, R., and Iaccarino, S., 2015, Tectonometamorphic discontinuities in the Greater Himalayan Sequence: A local or a regional feature?, *in* Mukherjee, S., Carosi, R., van der Beek, P.A., Mukherjee, B.K., and Robinson, D.M., eds., Tectonics of the Himalaya: Geological Society of London, Special Publications, v. 412, p. 25–41, https://doi.org/10.1144/SP412.3.

Murphy, M.A., 2007, Isotopic characteristics of the Gurla Mandhata metamorphic core complex: Implications for the architecture of the Himalayan orogen: Geology, v. 35, no. 11, p. 983–986, https://doi.org/10.1130/G23774A.1.

Murphy, M.A., and Copeland, P., 2005, Transtensional deformation in the central Himalaya and its role in accommodating growth of the Himalayan orogen: Tectonics, v. 24, no. 4, https://doi.org/10.1029/2004TC001659.

Murphy, M.A., and Yin, A., 2003, Structural evolution and sequence of thrusting in the Tethyan fold-thrust belt and Indus-Yalu suture zone, southwest Tibet: Geological Society of America Bulletin, v. 115, no. 1, p. 21–34, https://doi.org/10.1130/0016-7606(2003)115<0021:SEASOT>2.0.CO;2.

Murphy, M.A., Yin, A., Kapp, P., Harrison, M.T., Ding, L., and Guo, J., 2000, Southward propagation of the Karakoram fault system, southwest Tibet: Timing and magnitude of slip: Geology, v. 28, no. 5, p. 451–454, https://doi.org/10.1130/0091-7613(2000)28<451:SPOTKF>2.0.CO;2.

Murphy, M.A., Yin, A., Kapp, P., Harrison, T. M., Manning, C.E., Ryerson, F.J., Ding, L., and Guo, J.H., 2002, Structural evolution of the Gurla Mandhata detachment system, southwest Tibet: Implications for the eastward extent of the Karakoram fault system: Geological Society of America Bulletin, v. 114, no. 4, p. 428–447, https://doi.org/10.1130/0016-7606(2002)114<0428:SEOTGM>2.0.CO;2.

Murphy, M.A., Saylor, J.E., and Ding, L., 2009, Late Miocene topographic inversion in southwest Tibet based on integrated paleoelevation reconstructions and structural history: Earth and Planetary Science Letters, v. 282, no. 1–4, p. 1–9, https://doi.org/10.1016/j.epsl.2009.01.006.

Murphy, M.A., Taylor, M.H., Gosse, J., Silver, C.R.P., Whipp, D.M., and Beaumont, C., 2014, Limit of strain partitioning in the Himalaya marked by large earthquakes in western Nepal: Nature Geoscience, v. 7, no. 1, p. 38–42, https://doi.org/10.1038/ngeo2017.

Myrow, P.M., Hughes, N.C., Searle, M.P., Fanning, C.M., Peng, S.C., and Parcha, S.K., 2009, Stratigraphic correlation of Cambrian–Ordovician deposits along the Himalaya: Implications for the age and nature of rocks in the Mount Everest region: Geological Society of America Bulletin, v. 121, no. 3–4, p. 323–332, https://doi.org/10.1130/B26384.1.

Nagy, C., Godin, L., Antolín, B., Cottle, J., and Archibald, D., 2015, Mid-Miocene initiation of orogen-parallel extension, NW Nepal Himalaya: Lithosphere, v. 7, no. 5, p. 483–502, https://doi.org/10.1130/L425.1.

Oleskevich, D.A., Hyndman, R.D., and Wang, K., 1999, The updip and downdip limits to great subduction earthquakes: Thermal and structural models of Cascadia, south Alaska, SW Japan, and Chile: Journal of Geophysical Research. Solid Earth, v. 104, no. B7, p. 14965–14991, https://doi.org/10.1029/1999JB900060.

Pacheco, J.F., Sykes, L.R., and Scholz, C.H., 1993, Nature of seismic coupling along simple plate boundaries of the subduction type: Journal of Geophysical Research. Solid Earth, v. 98, no. B8, p. 14133–14159, https://doi.org/10.1029/93JB00349.

Pandey, M.R., Tandukar, R.P., Avouac, J.P., Lavé, J., and Massot, J.P., 1995, Interseismic strain accumulation on the Himalayan crustal ramp (Nepal): Geophysical Research Letters, v. 22, no. 7, p. 751–754, https://doi.org/10.1029/94GL02971.

Parsons, A.J., Ferré, E.C., Law, R.D., Lloyd, G.E., Phillips, R.J., and Searle, M.P., 2016, Orogen-parallel deformation of the Himalayan midcrust: Insights from structural and magnetic fabric analyses of the Greater Himalayan Sequence, Annapurna-Dhaulagiri Himalaya, central Nepal: Tectonics, https://doi.org/10.1002/2016TC004244.

Paudel, L., and Arita, K., 2002, Locating the Main Central Thrust in central Nepal using lithologic, microstructural and metamorphic criteria: Journal of Nepal Geological Society, v. 26, p. 29–42.

Pearson, O.N., and DeCelles, P.G., 2005, Structural geology and regional tectonic significance of the Ramgarh thrust, Himalayan fold-thrust belt of Nepal: Tectonics, v. 24, no. 4, https://doi.org/10.1029/2003TC001617.

Pêcher, A., 1989, The Metamorphism in the Central Himalaya: Journal of Metamorphic Geology, v. 7, no. 1, p. 31–41, https://doi.org/10.1111/j.1525-1314.1989.tb00573.x.

Pêcher, A., Bouchez, J.L., and Lefort, P., 1991, Miocene dextral shearing between Himalaya and Tibet: Geology, v. 19, no. 7, p. 683–685, https://doi.org/10.1130/0091-7613(1991)019<0683:MDSBHA>2.3.CO;2.

Phillips, R.J., Parrish, R.R., and Searle, M.P., 2004, Age constraints on ductile deformation and long-term slip rates along the Karakoram fault zone, Ladakh: Earth and Planetary Science Letters, v. 226, no. 3–4, p. 305–319, https://doi.org/10.1016/j.epsl.2004.07.037.

Platt, J.P., 1993, Mechanics of oblique convergence: Journal of Geophysical Research. Solid Earth, v. 98, no. B9, p. 16239–16256, https://doi.org/10.1029/93JB00888.

Pognante, U., and Benna, P., 1993, Metamorphic zonation, migmatization and leucogranites along the Everest transect of Eastern Nepal and Tibet: Record of an exhumation history, *in* Treloar, P.J., and Searle, M.P., eds., Himalayan Tectonics: Geological Society of London, Special Publications, v. 74, no. 1, p. 323–340, https://doi.org/10.1144/GSL.SP.1993.074.01.22.

Quidelleur, X., Grove, M., Lovera, O.M., Harrison, T.M., Yin, A., and Ryerson, F.J., 1997, Thermal evolution and slip history of the Renbu Zedong Thrust, southeastern Tibet: Journal of Geophysical Research. Solid Earth, v. 102, no. B2, p. 2659–2679, https://doi.org/10.1029/96JB02483.

Ratschbacher, L., Frisch, W., Liu, G., and Chen, C., 1994, Distributed deformation in southern and western Tibet during and after the India-Asia collision: Journal of Geophysical Research. Solid Earth, v. 99, no. B10, p. 19917–19945, https://doi.org/10.1029/94JB00932.

Robert, X., van der Beek, P., Braun, J., Perry, C., and Mugnier, J.L., 2011, Control of detachment geometry on lateral variations in exhumation rates in the Himalaya: Insights from low-temperature thermochronology and numerical modeling: Journal of Geophysical Research. Solid Earth, v. 116, no. B5, https://doi.org/10.1029/2010jb007893.

Robinson, D.M., and Martin, A.J., 2014, Reconstructing the Greater Indian margin: A balanced cross section in central Nepal focusing on the Lesser Himalayan duplex: Tectonics, v. 33, no. 11, p. 2143–2168, https://doi.org/10.1002/2014TC003564.

Robinson, D.M., and McQuarrie, N., 2012, Pulsed deformation and variable slip rates within the central Himalayan thrust belt: Lithosphere, v. 4, no. 5, p. 449–464, https://doi.org/10.1130/L204.1.

Robinson, D.M., DeCelles, P.G., Garzione, C.N., Pearson, O.N., Harrison, T.M., and Catlos, E.J., 2003, Kinematic model for the Main Central thrust in Nepal: Geology, v. 31, no. 4, p. 359–362, https://doi.org/10.1130/0091-7613(2003)031<0359:KMFTMC>2.0.CO;2.

Robinson, D.M., DeCelles, P.G., and Copeland, P., 2006, Tectonic evolution of the Himalayan thrust belt in western Nepal: Implications for channel flow models: Geological Society of America Bulletin, v. 118, no. 7–8, p. 865–885, https://doi.org/10.1130/B25911.1.

Ruff, L.J., and Tichelaar, B.W., 1996, What controls the seismogenic plate interface in subduction zones?, *in* Bebout, G.E., Scholl, D.W., Kirby, S.H., and Platt, J.P., eds., Subduction: Top to Bottom: American Geophysical Union Geophysical Monograph Series, v. 96, p. 105–111, https://doi.org/10.1029/GM096p0105.

Saylor, J., Quade, J., Dettman, D., DeCelles, P., Kapp, P., and Ding, L., 2009, The late Miocene through present paleoelevation history of southwestern Tibet: American Journal of Science, v. 309, no. 1, p. 1–42, https://doi.org/10.2475/01.2009.01.

Saylor, J., DeCelles, P., Gehrels, G., Murphy, M., Zhang, R., and Kapp, P., 2010, Basin formation in the High Himalaya by arc-parallel extension and tectonic damming: Zhada basin, southwestern Tibet: Tectonics, v. 29, no. 1, https://doi.org/10.1029/2008TC002390.

Schelling, D., and Arita, K., 1991, Thrust tectonics, crustal shortening, and the structure of the Far-Eastern Nepal Himalaya: Tectonics, v. 10, no. 5, p. 851–862, https://doi.org/10.1029/91TC01011.

Schill, E., Appel, E., Zeh, O., Singh, V.K., and Gautam, P., 2001, Coupling of late-orogenic tectonics and secondary pyrrhotite remanences: Towards a separation of different rotation processes and quantification of rotational underthrusting in the western Himalaya (northern India): Tectonophysics, v. 337, no. 1, p. 1–21, https://doi.org/10.1016/S0040-1951(01)00113-5.

Schill, E., Crouzet, C., Gautam, P., Singh, V.K., and Appel, E., 2002, Where did rotational shortening occur in the Himalayas?: Inferences from palaeomagnetic remagnetisations: Earth and Planetary Science Letters, v. 203, no. 1, p. 45–57, https://doi.org/10.1016/S0012-821X(02)00842-7.

Schill, E., Appel, E., Crouzet, C., Gautam, P., Wehland, F., and Staiger, M., 2004, Oroclinal bending versus regional significant clockwise rotations in the Himalayan arc: Constraints from secondary pyrrhotite remanences, *in* Sussman, A.J., and Weil, A.B., eds., Orogenic Curvature: Integrating Paleomagnetic and Structural Analyses: Geological Society of America Special Papers, v. 383, p. 73–85, https://doi.org/10.1130/0-8137-2383-3(2004)383[73:Obvrsc]2.0.CO;2.

Searle, M.P., 1999, Extensional and compressional faults in the Everest–Lhotse massif, Khumbu Himalaya, Nepal: Journal of the Geological Society, v. 156, no. 2, p. 227–240, https://doi.org/10.1144/gsjgs.156.2.0227.

Searle, M.P., and Godin, L., 2003, The South Tibetan Detachment and the Manaslu Leucogranite: A structural reinterpretation and restoration of the Annapurna-Manaslu Himalaya, Nepal: The Journal of Geology, v. 111, no. 5, p. 505–523, https://doi.org/10.1086/376763.

Searle, M.P., Simpson, R.L., Law, R.D., Parrish, R.R., and Waters, D.J., 2003, The structural geometry, metamorphic and magmatic evolution of the Everest massif, High Himalaya of Nepal-South Tibet: Journal of the Geological Society, v. 160, no. 3, p. 345–366, https://doi.org/10.1144/0016-764902-126.

Silver, C.R.P., Murphy, M.A., Taylor, M.H., Gosse, J., and Baltz, T., 2015, Neotectonics of the Western Nepal Fault System: Implications for Himalayan strain partitioning: Tectonics, v. 34, no. 12, p. 2494–2513, https://doi.org/10.1002/2014TC003730.

Soucy La Roche, R., and Godin, L., 2019, Inherited Cross-Strike Faults and Oligocene-Early Miocene Segmentation of the Main Himalayan Thrust, West Nepal: Journal of Geophysical Research. Solid Earth, v. 124, no. 7, p. 7429–7444, https://doi.org/10.1029/2019JB017467.

Srivastava, P., and Mitra, G., 1994, Thrust geometries and deep structure of the outer and lesser Himalaya, Kumaon and Garhwal (India): Implications for evolution of the Himalayan fold-and-thrust belt: Tectonics, v. 13, no. 1, p. 89–109, https://doi.org/10.1029/93TC01130.

Stevens, V.L., and Avouac, J.P., 2015, Interseismic coupling on the main Himalayan thrust: Geophysical Research Letters, v. 42, no. 14, p. 5828–5837, https://doi.org/10.1002/2015GL064845.

Styron, R.H., Taylor, M.H., and Murphy, M.A., 2011, Oblique convergence, arc-parallel extension, and the role of strike-slip faulting in the High Himalaya: Geosphere, v. 7, no. 2, p. 582–596, https://doi.org/10.1130/GES00606.1.

Subedi, S., Hetényi, G., Vergne, J., Bollinger, L., Lyon-Caen, H., Farra, V., Adhikari, L. B., and Gupta, R. M., 2018, Imaging the Moho and the Main Himalayan Thrust in Western Nepal with receiver functions: Geophysical Research Letters, v. 45, no. 24, p. 13222–13230, https://doi.org/10.1029/2018GL080911.

Suenaga, N., Yoshioka, S., Matsumoto, T., Manea, V.C., Manea, M., and Ji, Y., 2019, Two-dimensional thermal modeling of the Philippine Sea plate subduction in central Japan: Implications for gap of low-frequency earthquakes and tectonic tremors: Journal of Geophysi-

cal Research. Solid Earth, v. 124, no. 7, p. 6848–6865, https://doi.org/10.1029/2018JB017068.

Thiede, R.C., Arrowsmith, J.R., Bookhagen, B., McWilliams, M., Sobel, E.R., and Strecker, M.R., 2006, Dome formation and extension in the Tethyan Himalaya, Leo Pargil, northwest India: Geological Society of America Bulletin, v. 118, no. 5–6, p. 635–650, https://doi.org/10.1130/B25872.1.

Thöni, M., Miller, C., Hager, C., Grasemann, B., and Horschinegg, M., 2012, New geochronological constraints on the thermal and exhumation history of the Lesser and Higher Himalayan Crystalline Units in the Kullu-Kinnaur area of Himachal Pradesh (India): Journal of Asian Earth Sciences, v. 52, no. 3, p. 98–116, https://doi.org/10.1016/j.jseaes.2012.02.015.

Valli, F., Arnaud, N., Leloup, P.H., Sobel, E.R., Mahéo, G., Lacassin, R., Guillot, S., Li, H., Tapponnier, P., and Xu, Z., 2007, Twenty million years of continuous deformation along the Karakorum fault, western Tibet: A thermochronological analysis: Tectonics, v. 26, no. 4, https://doi.org/10.1029/2005TC001913.

van der Beek, P., Litty, C., Baudin, M., Mercier, J., Robert, X., and Hardwick, E., 2016, Contrasting tectonically driven exhumation and incision patterns, western versus central Nepal Himalaya: Geology, v. 44, no. 4, p. 327–330, https://doi.org/10.1130/G37579.1.

Vannay, J.C., and Steck, A., 1995, Tectonic evolution of the High Himalaya in Upper Lahul (NW Himalaya, India): Tectonics, v. 14, no. 2, p. 253–263, https://doi.org/10.1029/94TC02455.

Vannay, J.C., and Hodges, K.V., 1996, Tectonometamorphic evolution of the Himalayan metamorphic core between the Annapurna and Dhaulagiri, central Nepal: Journal of Metamorphic Geology, v. 14, no. 5, p. 635–656, https://doi.org/10.1046/j.1525-1314.1996.00426.x.

Wang, C., Gao, R., Yin, A., Wang, H., Zhang, Y., Guo, T., Li, Q., and Li, Y., 2011, A mid-crustal strain-transfer model for continental deformation: A new perspective from high-resolution deep seismic-reflection profiling across NE Tibet: Earth and Planetary Science Letters, v. 306, no. 3, p. 279–288, https://doi.org/10.1016/j.epsl.2011.04.010.

Wang, J.M., Wu, F.Y., Rubatto, D., Liu, K., Zhang, J.J., and Liu, X.C., 2018, Early Miocene rapid exhumation in southern Tibet: insights from P–T–t–D–magmatism path of Yardoi dome: Lithos, v. 304–307, p. 38–56, https://doi.org/10.1016/j.lithos.2018.02.003.

Wang, K., and Hu, Y., 2006, Accretionary prisms in subduction earthquake cycles: The theory of dynamic Coulomb wedge: Journal of Geophysical Research. Solid Earth, v. 111, no. B6, https://doi.org/10.1029/2005jb004094.

Wang, S., Zhang, W., Fang, X., Dai, S., and Kempf, O., 2008, Magnetostratigraphy of the Zanda basin in southwest Tibet Plateau and its tectonic implications: Chinese Science Bulletin, v. 53, no. 1393, https://doi.org/10.1007/s11434-008-0132-9.

Wang, X., Wei, S., and Wu, W., 2017, Double-ramp on the Main Himalayan Thrust revealed by broadband waveform modeling of the 2015 Gorkha earthquake sequence: Earth and Planetary Science Letters, v. 473, p. 83–93, https://doi.org/10.1016/j.epsl.2017.05.032.

Webb, A.A.G., 2013, Preliminary balanced palinspastic reconstruction of Cenozoic deformation across the Himachal Himalaya (northwestern India): Geosphere, v. 9, no. 3, p. 572–587, https://doi.org/10.1130/GES00787.1.

Webb, A.A.G., Yin, A., Harrison, T.M., Célérier, J., and Burgess, W.P., 2007, The leading edge of the Greater Himalayan Crystalline complex revealed in the NW Indian Himalaya: Implications for the evolution of the Himalayan orogen: Geology, v. 35, no. 10, p. 955–958, https://doi.org/10.1130/G23931A.1.

Webb, A.A.G., Yin, A., Harrison, T.M., Celerier, J., Gehrels, G.E., Manning, C.E., and Grove, M., 2011, Cenozoic tectonic history of the Himachal Himalaya (northwestern India) and its constraints on the formation mechanism of the Himalayan orogen: Geosphere, v. 7, no. 4, p. 1013–1061, https://doi.org/10.1130/GES00627.1.

Whipp, D., and Beaumont, C., 2016, Orogen-parallel mass transport along the arcuate Himalaya into Nanga Parbat and the western Himalayan syntaxis: European Geosciences Union, General Assembly Conference Abstracts, Vienna, Austria, 17–22 April, v. 19.

Whipp, D.M., Jr., and Ehlers, T.A., 2007, Influence of groundwater flow on thermochronometer-derived exhumation rates in the central Nepalese Himalaya: Geology, v. 35, no. 9, p. 851–854, https://doi.org/10.1130/G23788A.1.

Whipp, D.M., Beaumont, C., and Braun, J., 2014, Feeding the "aneurysm": Orogen-parallel mass transport into Nanga Parbat and the western Himalayan syntaxis: Journal of Geophysical Research. Solid Earth, v. 119, no. 6, p. 5077–5096, https://doi.org/10.1002/2013JB010929.

Whipple, K.X., Shirzaei, M., Hodges, K.V., and Ramon Arrowsmith, J., 2016, Active shortening within the Himalayan orogenic wedge implied by the 2015 Gorkha earthquake: Nature Geoscience, v. 9, no. 9, p. 711–716, https://doi.org/10.1038/ngeo2797.

Wiesmayr, G., and Grasemann, B., 2002, Eohimalayan fold and thrust belt: Implications for the geodynamic evolution of the NW-Himalaya (India): Tectonics, v. 21, no. 6, p. 8-1–8-18, https://doi.org/10.1029/2002TC001363.

Wobus, C., Whipple, K.X., Kirby, E., Snyder, N., Johnson, J., Spyropolou, K., Crosby, B., and Sheehan, D., 2006, Tectonics from topography: Procedures, promise, and pitfalls, *in* Willett, S.D., Hovius, N., Brandon, M.T., Fisher, D.M., eds., Tectonics, Climate, and Landscape Evolution: Geological Society of America Special Papers, v. 398, p. 55–74, https://doi.org/10.1130/2006.2398(04).

Xu, Z., Wang, Q., Pêcher, A., Liang, F., Qi, X., Cai, Z., Li, H., Zeng, L., and Cao, H., 2013, Orogen-parallel ductile extension and extrusion of the Greater Himalaya in the late Oligocene and Miocene: Tectonics, v. 32, no. 2, p. 191–215, https://doi.org/10.1002/tect.20021.

Yakymchuk, C., and Godin, L., 2012, Coupled role of deformation and metamorphism in the construction of inverted metamorphic sequences: An example from far-northwest Nepal: Journal of Metamorphic Geology, v. 30, no. 5, p. 513–535, https://doi.org/10.1111/j.1525-1314.2012.00979.x.

Yin, A., 2006, Cenozoic tectonic evolution of the Himalayan orogen as constrained by along-strike variation of structural geometry, exhumation history, and foreland sedimentation: Earth-Science Reviews, v. 76, no. 1–2, p. 1–131, https://doi.org/10.1016/j.earscirev.2005.05.004.

Yin, A., Harrison, T.M., Ryerson, F.J., Chen, W.J., Kidd, W.S.F., and Copeland, P., 1994, Tertiary structural evolution of the Gangdese Thrust System, southeastern Tibet: Journal of Geophysical Research. Solid Earth, v. 99, no. B9, p. 18175–18201, https://doi.org/10.1029/94JB00504.

Yin, A., Harrison, M.T., Murphy, M.A., Grove, M., Nie, S., Ryerson, F., Wang, X.F., and Chen, Z.L., 1999, Tertiary deformation history of southeastern and southwestern Tibet during the Indo-Asian collision: Geological Society of America Bulletin, v. 111, no. 11, p. 1644–1664, https://doi.org/10.1130/0016-7606(1999)111<1644:TDHOSA>2.3.CO;2.

Zhang, J., Ding, L., Zhong, D., and Zhou, Y., 2000, Orogen-parallel extension in Himalaya: Is it the indicator of collapse or the product in process of compressive uplift?: Chinese Science Bulletin, v. 45, no. 2, p. 114–120, https://doi.org/10.1007/BF02884653.

Zhang, R., Murphy, M.A., Lapen, T.J., Sanchez, V., and Heizler, M., 2011, Late Eocene crustal thickening followed by Early-Late Oligocene extension along the India-Asia suture zone: Evidence for cyclicity in the Himalayan orogen: Geosphere, v. 7, no. 5, p. 1249–1268, https://doi.org/10.1130/GES00643.1.

Zhang, Y., Wang, R., Walter, T.R., Feng, W., Chen, Y., and Huang, Q., 2017, Significant lateral dip changes may have limited the scale of the 2015 M_w 7.8 Gorkha earthquake: Geophysical Research Letters, v. 44, no. 17, p. 8847–8856, https://doi.org/10.1002/2017GL074095.

Science Editor: Rob Strachan
Associate Editor: Bernhard Grasemann

Manuscript Received 15 October 2019
Revised Manuscript Received 23 February 2020
Manuscript Accepted 20 March 2020

Printed in the USA